

Article

Chemotaxis shapes the microscale organization of the ocean's microbiome

<https://doi.org/10.1038/s41586-022-04614-3>

Received: 12 June 2020

Accepted: 4 March 2022

Published online: 20 April 2022

 Check for updates

Jean-Baptiste Raina¹✉, Bennett S. Lambert^{2,3,4,5}, Donovan H. Parks⁶, Christian Rinke⁶, Nachshon Siboni¹, Anna Bramucci¹, Martin Ostrowski¹, Brandon Signal¹, Adrian Lutz⁷, Himasha Mendis⁷, Francesco Rubino⁶, Vicente I. Fernandez⁵, Roman Stocker⁵, Philip Hugenholtz⁶, Gene W. Tyson^{6,8} & Justin R. Seymour¹✉

The capacity of planktonic marine microorganisms to actively seek out and exploit microscale chemical hotspots has been widely theorized to affect ocean-basin scale biogeochemistry^{1–3}, but has never been examined comprehensively *in situ* among natural microbial communities. Here, using a field-based microfluidic platform to quantify the behavioural responses of marine bacteria and archaea, we observed significant levels of chemotaxis towards microscale hotspots of phytoplankton-derived dissolved organic matter (DOM) at a coastal field site across multiple deployments, spanning several months. Microscale metagenomics revealed that a wide diversity of marine prokaryotes, spanning 27 bacterial and 2 archaeal phyla, displayed chemotaxis towards microscale patches of DOM derived from ten globally distributed phytoplankton species. The distinct DOM composition of each phytoplankton species attracted phylogenetically and functionally discrete populations of bacteria and archaea, with 54% of chemotactic prokaryotes displaying highly specific responses to the DOM derived from only one or two phytoplankton species. Prokaryotes exhibiting chemotaxis towards phytoplankton-derived compounds were significantly enriched in the capacity to transport and metabolize specific phytoplankton-derived chemicals, and displayed enrichment in functions conducive to symbiotic relationships, including genes involved in the production of siderophores, B vitamins and growth-promoting hormones. Our findings demonstrate that the swimming behaviour of natural prokaryotic assemblages is governed by specific chemical cues, which dictate important biogeochemical transformation processes and the establishment of ecological interactions that structure the base of the marine food web.

Understanding how organisms forage within a heterogeneous resource landscape is a fundamental goal of ecology⁴. In the ocean, populations of microorganisms govern marine productivity and biogeochemical cycling over vast, ocean basin scales^{5,6}. However, from the perspective of an individual planktonic microbe, important ecological processes including resource acquisition⁷, predation and symbiosis occur over microscopic scales, often within a surprisingly heterogeneous seascape shaped by microscale gradients of chemical resources and foraging cues^{3,8}. Evidence from theoretical and laboratory-based studies indicate that some marine microbes are highly adept at foraging within patchy environments using chemotactic behaviour^{9–11}—the capacity to migrate up or down chemical gradients—and that these behaviours may have important ecological and biogeochemical implications^{12–14}.

Microbial chemotaxis has been studied primarily in highly structured microenvironments such as biofilms, soil or host tissues¹⁵. However, this behaviour might also have important roles in the ocean water column, enabling bacteria to exploit localized nutrient hotspots¹⁶, colonize particles¹⁴ or establish spatial associations with other microorganisms¹⁷ such as phytoplankton¹⁸. For instance, it has been proposed that chemotaxis enables bacteria to colonize the microenvironment surrounding individual phytoplankton cells, called the phycosphere¹⁹, which is characterized by pronounced gradients of DOM^{18,20}. Chemotaxis may be critical for microbes to establish and maintain the close spatial association required for reciprocal chemical exchanges to occur within the phycosphere, which can enhance the growth of both the bacterial and phytoplankton partners²¹ and ultimately influence the productivity of marine ecosystems¹⁸. Although the role of chemotaxis

¹Climate Change Cluster, Faculty of Science, University of Technology Sydney, Ultimo, New South Wales, Australia. ²Ralph M. Parsons Laboratory, Department of Civil and Environmental Engineering, Massachusetts Institute of Technology, Cambridge, MA, USA. ³Department of Applied Ocean Physics and Engineering, Woods Hole Oceanographic Institution, Woods Hole, MA, USA. ⁴Center for Environmental Genomics, School of Oceanography, University of Washington, Seattle, WA, USA. ⁵Department of Civil, Environmental and Geomatic Engineering, ETH Zurich, Zurich, Switzerland. ⁶Australian Centre for Ecogenomics, School of Chemistry and Molecular Biosciences, The University of Queensland, St Lucia, Queensland, Australia. ⁷Metabolomics Australia, Bio21 Institute, The University of Melbourne, Parkville, Victoria, Australia. ⁸Centre for Microbiome Research, School of Biomedical Sciences, Translational Research Institute, Queensland University of Technology, Woolloongabba, Queensland, Australia. ✉e-mail: Jean-Baptiste.Raina@uts.edu.au; Justin.Seymour@uts.edu.au

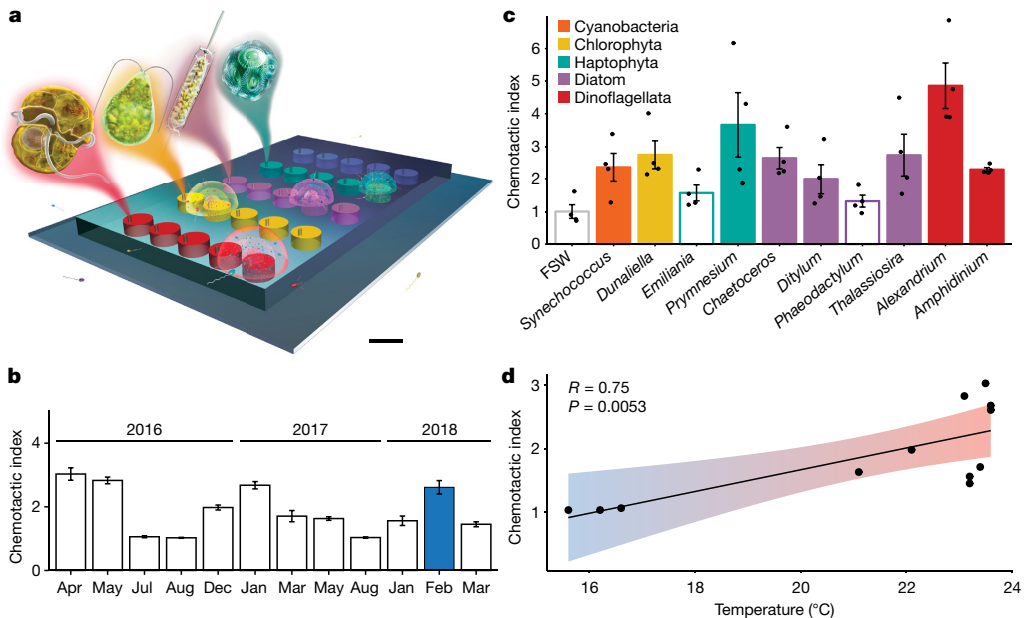


Fig. 1 | Use of ISCA to probe for chemotaxis towards phytoplankton-derived DOM in the natural environment. **a**, Phytoplankton-derived DOM is loaded in ISCA wells before deployment in the ocean. Each well is independently connected to the external environment by a port, through which chemicals can diffuse and microorganisms can enter. Upon deployment, the ISCA produces chemical microplumes that mimic microscale nutrient hotspots. Chemotactic prokaryotes respond by swimming into the ISCA wells and can then be counted by flow cytometry and characterized by microscale metagenomics. Scale bar, 7.5 mm. **b**, Average I_c elicited by the phytoplankton-derived DOM over a 2 year period at Clovelly Beach (33.91°S, 151.26°E). I_c denotes the concentration of cells in ISCA wells, normalized by the mean concentration of cells in wells containing filtered seawater ($n=10$). The full dataset is presented in

Supplementary Figure 1. The blue bar represents the ISCA experiment (February 2018) that was further analysed using metagenomics and metabolomics. Data are mean \pm s.e.m. **c**, Details of the I_c across the 10 different phytoplankton-derived DOM treatments in February 2018 (normalized by the mean concentration of cells within wells containing filtered seawater) after 60 min field deployment. Solid bars are significantly different from wells containing filtered seawater (ANOVA (one-sided), $n=4$, $P<0.05$; P -values are reported in Supplementary Table 3). Each treatment was replicated across four different ISCAs ($n=4$). Data are mean \pm s.e.m. **d**, Significant correlation between I_c (presented in **b**) and temperature (Pearson's correlation (two-sided), $P=0.0053$). The 95% confidence interval of the correlation coefficient is displayed. Artwork: Glynn Gorick.

in marine systems has been explored extensively in model systems in laboratory settings, there is currently little evidence that natural communities of marine bacteria and archaea use these behaviours *in situ* and our understanding of the chemical currencies that drive these behaviours in the environment is limited.

To determine whether natural assemblages of marine microbes can use chemotaxis to exploit a patchy chemical seascape and to examine the behavioural, chemical and genomic features regulating interactions between phytoplankton and prokaryotes, we used the *in situ* chemotaxis assay²² (ISCA). This microfluidic platform comprises a parallelized array of micro-wells, each connected to the outside seawater by a port²². When deployed in the ocean, chemoattractants pre-loaded in each well diffuse into the surrounding seawater, creating microscale chemical plumes analogous to those resulting from diffusing hotspots, such as the phycosphere (Fig. 1a). Chemotactic microorganisms in the surrounding water column migrate up the chemical gradients towards the source of the plume and become trapped inside the well. We used the ISCA to simulate phycospheres and measure the behavioural responses of planktonic prokaryotes to phytoplankton-derived DOM hotspots, and then characterized the genomic and biochemical basis for these responses by analysing the identity and metabolic capacity of microorganisms trapped in the wells. Using this *in situ* approach, we tested the hypotheses that (1) chemotaxis is pervasive among natural assemblages of marine bacteria and archaea, enabling them to exploit localized chemical hotspots such as the phycosphere; and (2) differences in chemical composition between phytoplankton-derived DOM underpin selectivity in behavioural responses, leading to taxonomic and functional partitioning of prokaryotic communities at the ocean's microscale.

DOM was collected from a total of 14 marine phytoplankton species, spanning globally abundant and ecologically important groups (diatoms, dinoflagellates, haptophytes, cryptophytes, chlorophytes and cyanobacteria), which occur in the coastal surface waters of eastern Australia (Supplementary Table 1). ISCA wells were loaded with phytoplankton-derived DOM (phytoplankton-DOM) or filtered seawater from the deployment site (which acted as a control) and were deployed for 1 h in surface waters (1 m depth) in 12 independent experiments, performed over 2 years at a coastal site near Sydney, Australia. Each treatment was replicated across four different ISCAs that were deployed simultaneously ($n=4$). Following deployment, the contents of the ISCA wells were retrieved and flow cytometry was used to enumerate microbial cells, enabling quantification of the strength of chemotaxis towards the DOM of each phytoplankton species, which was defined by the chemotactic index (I_c), equivalent to the number of cells in a treatment divided by the average number of cells in the control wells²².

In situ chemotaxis assays

ISCA experiments revealed that natural populations of marine prokaryotes exhibited strong chemotaxis towards the chemicals produced by phytoplankton (analysis of variance (ANOVA), $P<0.05$; Fig. 1a–c, Extended Data Fig. 1, Supplementary Table 3). Chemotactic strength varied considerably between ISCA deployments (Fig. 1b, Extended Data Fig. 1) and exhibited a significant and positive correlation with water temperature (Pearson's $R=0.75$, $P<0.01$; Fig. 1d, Extended Data Fig. 2). Chemotaxis was not detected during the three ISCA deployments carried out during austral winter months, potentially owing to the lower numbers of motile cells in winter⁸, slower swimming speed in colder water²³, or other biological factors (for example, protozoan grazing or

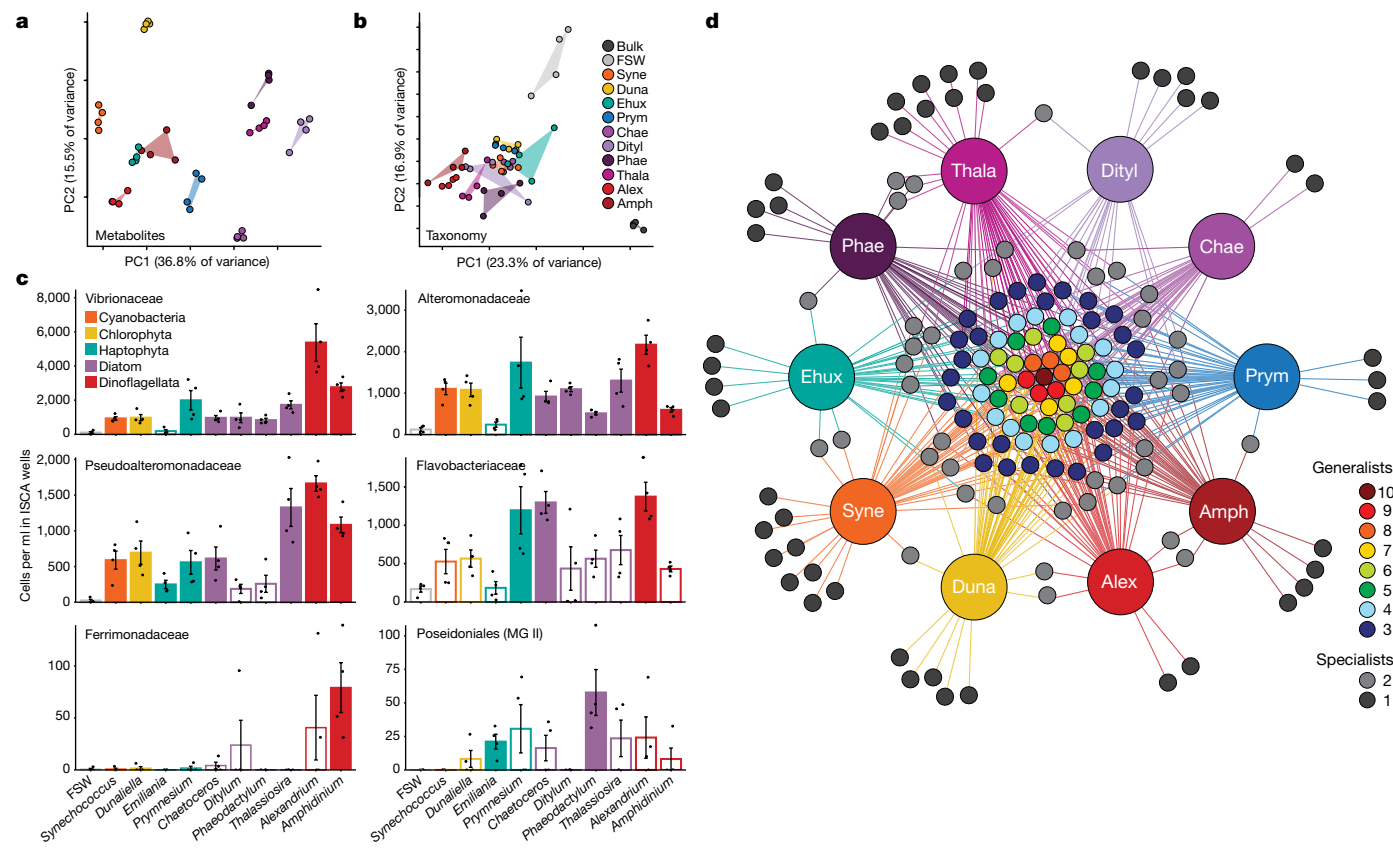


Fig. 2 | ‘Generalist’ and ‘specialist’ prokaryotic taxa responding to phytoplankton-DOM. **a**, Principal component analysis (PCA) of the chemical composition of phytoplankton-derived DOM. The first two components (PCs) account for 52.3% of the total variance. **b**, PCA of prokaryotic taxonomic composition (16S rRNA gene) of the bulk seawater (dark grey), filtered seawater (FSW) controls (grey) and phytoplankton-derived DOM. The first two components account for 40.2% of the total variance. **c**, Absolute abundance of selected ‘generalists’ (responding significantly to more than two different phytoplankton-derived DOM; top four graphs) and ‘specialists’ (significantly enriched in only one or two phytoplankton-derived DOM; bottom two graphs) in ISCA wells, grouped at the family level. Solid bars indicate significant differences from wells containing filtered seawater (ANOVA (one-sided), $n = 4$, $P < 0.05$; P -values are reported in Supplementary Table 6). For the full list of significantly enriched taxa see Supplementary Table 6. Data are mean \pm s.e.m.

viral lysis). In summer and autumn, DOM from the dinoflagellate *Amphidinium* elicited significant chemotactic responses in 8 out of 9 (88.8%) ISCA deployments, with I_c values of up to 4.6 ± 0.9 (corresponding to 4.6 times more cells than in the controls; Extended Data Fig. 1, Supplementary Table 3), whereas the diatoms *Ditylum* and *Thalassiosira* and the chlorophyte *Dunaliella*, elicited significant chemotactic responses in 7 out of 9 (77.7%) deployments. These results provide in situ evidence that natural assemblages of marine prokaryotes have the capacity to sense and respond to microscale patches of phytoplankton-derived DOM in the water column.

Some of the strongest chemotactic responses were recorded in February 2018, and these samples were selected for detailed analysis using metabolomics and microscale metagenomics²⁴. During this deployment, the DOM of 8 of the 10 phytoplankton species promoted positive chemotaxis (ANOVA, $P < 0.05$; Fig. 1b, Supplementary Table 3). The strongest chemotactic responses were recorded for DOM derived from the dinoflagellate *Alexandrium minutum* and the haptophyte *Prymnesium parvum*, with I_c values of 4.8 ± 0.8 and 3.6 ± 0.9 , respectively. DOM derived from *Synechococcus*, *Dunaliella*, *Chaetoceros*, *Thalassiosira* and *Amphidinium* elicited I_c values between 2.3 and 2.7.

d, Network analysis showing the differentiation between ‘generalist’ and ‘specialist’ taxa. Chemotactic prokaryotic taxa (small circles; nodes) are linked to the phytoplankton-DOM treatments they significantly responded to (large circles) by lines (edges) coloured according to each treatment. The colour of each node corresponds to the number of phytoplankton treatments they are significantly enriched in (see Extended Data Fig. 5, Supplementary Table 6 for taxonomic information). If a prokaryotic taxon responded only to one or two treatments, its corresponding node appears in grey at the periphery of the network. If a prokaryotic taxon responded to three or more treatments, its corresponding node appears towards the centre in a colour ranging from blue to brown. Alex, *Alexandrium*; Amph, *Amphidinium*; Chae, *Chaetoceros*; Dityl, *Ditylum*; Duna, *Dunaliella*; Ehux, *Emiliania*; Phae, *Phaeodactylum*; Prym, *Prymnesium*; Syne, *Synechococcus*; Thala, *Thalassiosira*.

The DOM derived from each phytoplankton species displayed distinct chemical fingerprints (Fig. 1, Extended Data Fig. 3, Supplementary Table 4), consistent with previous reports showing that marine phytoplankton can release characteristic suites of organic material²⁵. A total of 111 phytoplankton-derived compounds were detected from the water-soluble fraction of the collected DOM, consisting primarily of amino acids, amines, sugars, organic acids, fatty acids and other metabolic intermediates (Fig. 2a, Extended Data Fig. 3). These results indicate that variability in the extent of chemotactic responses was governed by the chemical composition of the different phytoplankton-derived DOM.

Identity of attracted prokaryotes

Microscale metagenomic analysis²⁴ revealed that phytoplankton-DOM treatments attracted specific microbial communities that were significantly different from both those present in the filtered seawater control and those present in the surrounding seawater at the deployment site (PERMANOVA, $P < 0.05$; Fig. 2b, Extended Data Fig. 4, Supplementary Table 5). In addition, the microbial communities present in the ten

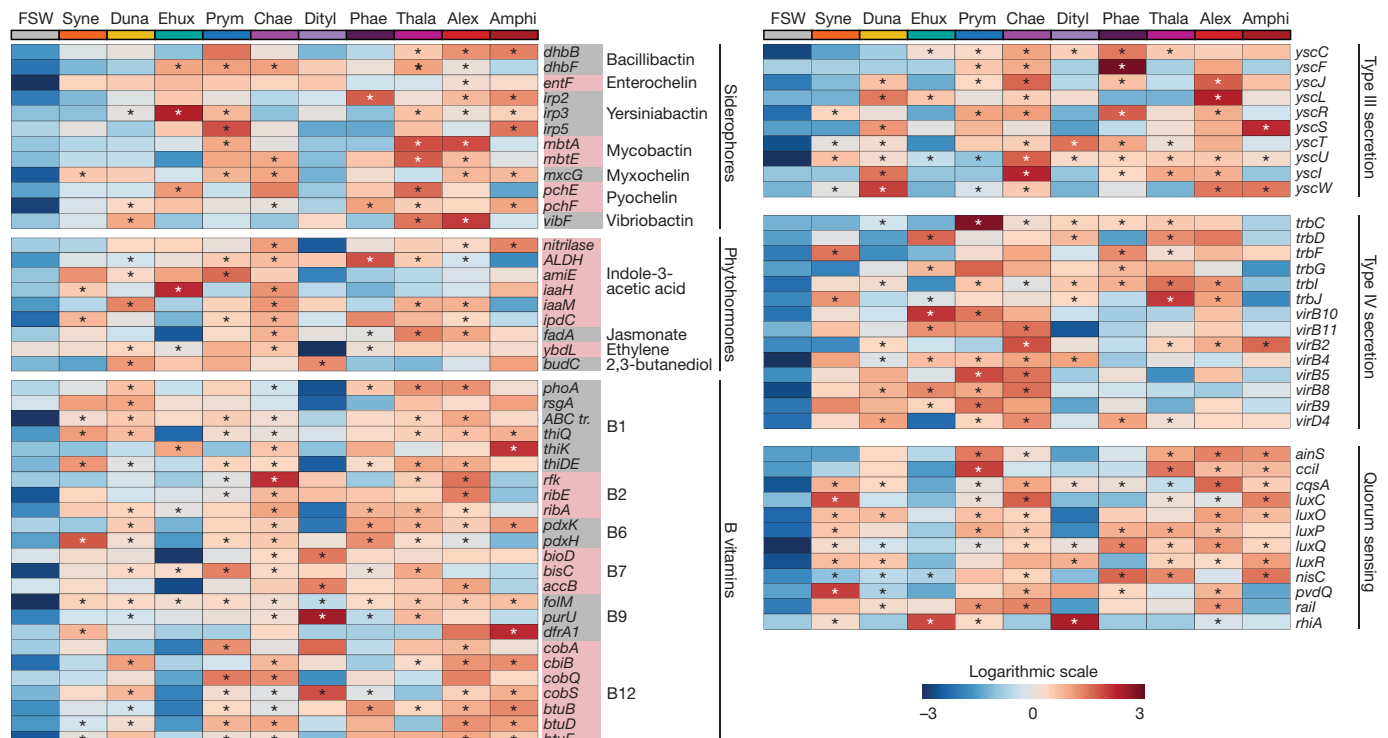


Fig. 3 | Enrichment of prokaryotic genes involved in phytoplankton–bacteria interactions. Genes involved in B vitamin, siderophore and phytohormone biosynthesis, quorum sensing and type III and IV secretion system assembly were significantly enriched in the prokaryotic communities responding to phytoplankton-derived DOM. Data were log-transformed and

mean-centred (generalized logarithm; $n = 4$) for each ISCA treatment. Sets of product-specific genes are distinguished by red and grey shading in the left panel. The full list of genes significantly enriched in phytoplankton–DOM can be found in Supplementary Table 8.

phytoplankton–DOM treatments were significantly different to each other (PERMANOVA, $P < 0.05$). We identified 163 taxa belonging to 27 bacterial and 2 archaeal phyla, which were significantly enriched (F -tests, $P < 0.05$, Supplementary Table 6) in ISCA wells containing phytoplankton-derived DOM relative to the control. The most highly enriched species belonged to the Vibrionaceae, Alteromonadaceae and Pseudoalteromonadaceae, with the absolute abundance of these highly motile and chemotactic bacterial families²⁰ up to 60-fold higher in DOM derived from the dinoflagellate *Alexandrium tamarense* compared with the control (Fig. 2c). Approximately half (46%) of the significantly enriched taxa responded to DOM from 3 or more phytoplankton species, indicating a generalist response to phytoplankton-derived DOM (Fig. 2d, Extended Data Fig. 5, Supplementary Table 6). Among the generalist taxa, populations of the Gammaproteobacteria genera *Pseudoalteromonas*, *Thalassomonas* and *Vibrio* were significantly enriched in 9 out of 10 phytoplankton-derived DOM (Extended Data Fig. 5). The other half (54%) of the significantly enriched taxa responded to DOM from only 1 (29%) or 2 (25%) phytoplankton species, indicating a more specialist chemotactic response (Fig. 2d, Extended Data Fig. 5, Supplementary Table 6). These specialist groups included the Alphaproteobacteria genera *Novispirillum*, *Dinoroseobacter* and *Octadecabacter*, and the Bacteroidia genera *Maribacter* and *Aquimarina* (Extended Data Fig. 5). These results suggest that specialist chemotactic responses promote the establishment of specific associations between phytoplankton and prokaryotes, ultimately driving microscale partitioning in the composition of marine microbial assemblages.

Functions of attracted prokaryotes

In addition to being taxonomically different, the bacterial and archaeal populations that exhibited chemotaxis to phytoplankton-derived DOM were also functionally distinct from those in the filtered seawater

controls (which represent prokaryote populations that enter the ISCA wells via random motility without using chemotaxis) and surrounding seawater (PERMANOVA, $P < 0.05$; Supplementary Table 7). As expected, all ISCA treatments, including the filtered seawater controls, were significantly enriched in genes involved in motility and chemotaxis (such as *che*, *flg* and *fli*; F -tests, $P < 0.05$; Extended Data Fig. 6), but also in genes mediating surface attachment (such as *cpa* and *pil*; F -tests, $P < 0.05$). Notably, several functions that promote beneficial interactions with phytoplankton, including production of siderophores, plant growth-promoting hormones and vitamins, as well as quorum sensing and secretion systems, were enriched in prokaryotes responding to phytoplankton-derived DOM (Fig. 3).

Functional orthologues involved in the production of siderophores, including Mycobactin and Vibriobactin, were significantly enriched in prokaryotes responding to phytoplankton–DOM compared with controls (F -tests, $P < 0.05$; Supplementary Table 8). Siderophores are small compounds excreted by bacteria and archaea that have high affinity for iron and increase its solubility and bioavailability²⁶. Iron limits primary production in vast areas of the world ocean²⁷, but phytoplankton can gain access to this essential micronutrient through bacterial siderophores²⁸, which have been proposed to promote phytoplankton–bacteria mutualism²⁹. The observed enrichment of siderophore-related genes in responding prokaryotic populations raises the prospect that some phytoplankton may release specific chemical cues to attract chemotactic siderophore-producing bacteria into their phycosphere.

Genes required for the biosynthesis of the plant growth-promoting hormones indole-3-acetic acid, jasmonate, ethylene, 2,3-butanediol, as well as multiple B vitamins (thiamine (vitamin B₁) and cobalamin (vitamin B₁₂)) were significantly enriched in prokaryotes responding to phytoplankton-derived DOM (F -tests, $P < 0.05$; Supplementary Table 8). For example, orthologues involved in the production and transport of

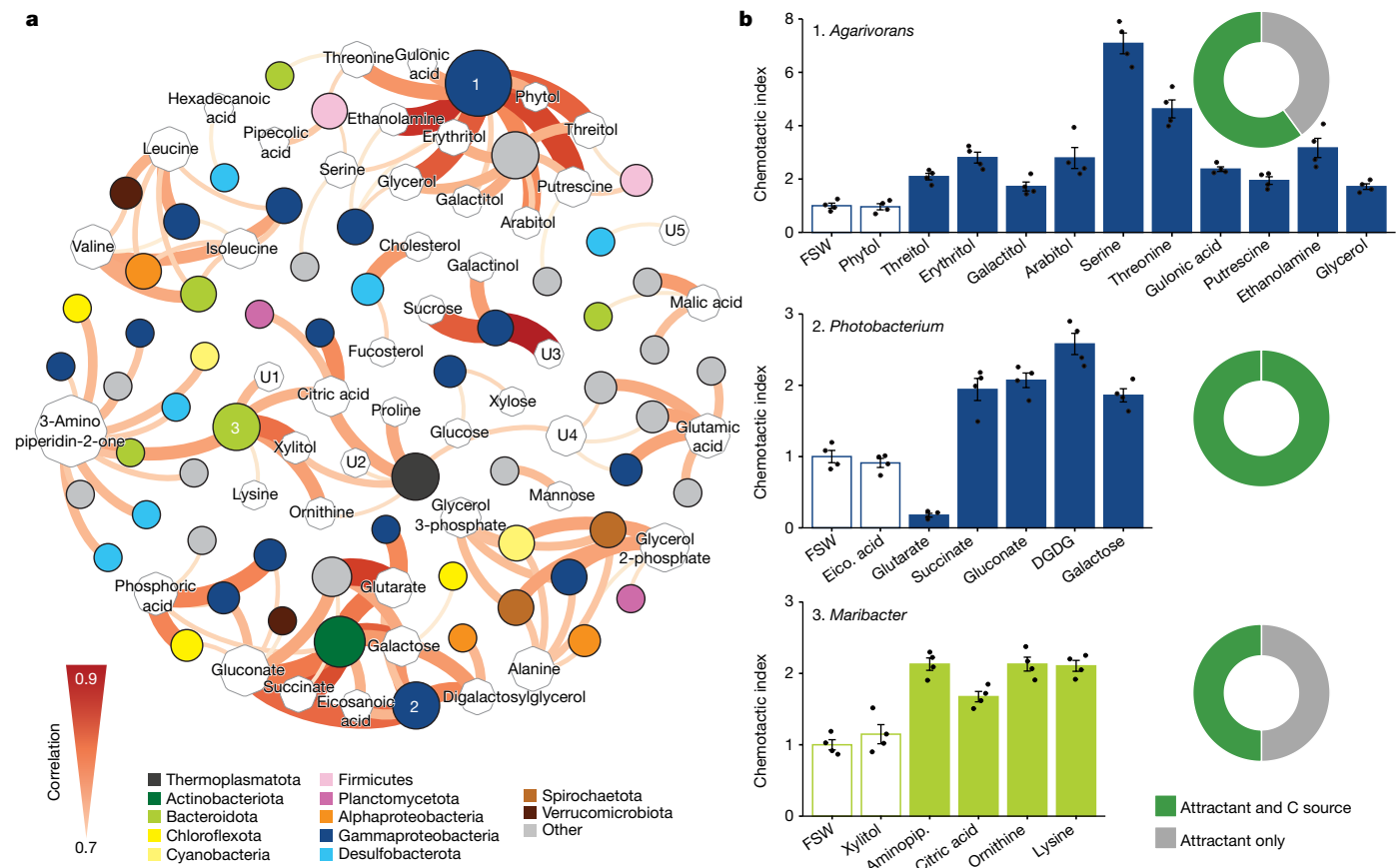


Fig. 4 | Specific associations between prokaryotes and phytoplankton-derived metabolites. **a**, Network analysis showing the positive correlations between specific compounds and prokaryotic taxa. Chemotactic prokaryotic taxa (circles; nodes) are linked to the chemicals they responded to (octagons) by lines (proportional in colour and thickness to the strength of the correlation, ranging from 0.7 to 0.9). Out of 112,110 possible correlations (111 compounds and 1,010 taxa), only 131 were significant (all displayed here) and all of them were positive. Because of this conservative approach, many potential links between taxa and compounds were excluded. **b**, To test the validity of this correlative approach, laboratory-based chemotaxis assays were carried out on isolates of three of the most prevalent

prokaryotic nodes from the network (presented in **a**): *Agarivorans albus*, *Photobacterium* sp. and *Maribacter dokdonensis*. Solid bars are significantly different from wells containing filtered seawater (ANOVA (one-sided), $n=4$, $P<0.05$; P -values are reported in Supplementary Table 9). Data are mean \pm s.e.m. Eico. acid, eicosanoic acid; DGDG, digalactosyldiacylglycerol; 3-aminopip., 3-aminopiperidin-2-one. In total, 18 out of 22 compounds tested (81.8%) attracted the isolates. The donut charts indicate the proportion of chemoattractants also used as carbon sources by each isolate; in total 12 out of 18 chemoattractants (66.6%) were also used as a carbon source (see Supplementary Fig. 10 for more details).

thiamine were on average 2.3 ± 0.5 times more abundant in communities exhibiting chemotaxis towards phytoplankton-derived DOM compared with controls (Fig. 3). Most phytoplankton are auxotrophs for essential cofactors such as B vitamins, and are completely reliant on prokaryotic production to fulfil their needs^{30,31}. In addition, prokaryotic production of growth-promoting hormones is common among soil bacteria associated with the rhizosphere of terrestrial plants³² and has been observed in bacteria within diatom cultures, where these molecules have been proposed to affect phytoplankton cell division and productivity²¹. B vitamins and growth-promoting hormones have therefore been predicted to be key currencies of chemical transactions between phytoplankton and bacteria¹⁸ and the enrichment of genes involved in their production in phytoplankton–DOM-containing ISCA wells provides evidence that chemotactic prokaryotes that colonize phycosphere play a critical role in supporting phytoplankton growth and metabolism.

Genes encoding type III and IV secretion systems were on average 50.1 ± 5.1 and 2.5 ± 0.7 times more abundant in phytoplankton–DOM treatments compared with controls, respectively (F -tests, $P<0.05$; Supplementary Table 8). These large protein complexes enable bacterial translocation of molecules and have been studied primarily in the context of pathogenic interactions^{33,34}, but bacterial symbionts also use

these molecular mechanisms to efficiently transfer specific compounds to their hosts³⁵. For example, type IV secretion systems are present in the genomes of nearly half of the most common phytoplankton-associated *Roseobacters*³⁶. The abundance of secretion system genes in prokaryotes attracted by phytoplankton-derived DOM suggests that phycosphere microbes may use them to facilitate the exchange of metabolites between cells. Finally, genes required to produce quorum-sensing molecules were also significantly enriched in phytoplankton–DOM treatments (F -tests, $P<0.05$; Supplementary Table 8). Quorum sensing has been predicted to regulate phytoplankton–bacteria interactions by mediating surface attachment³⁷ and the colonization of the phycosphere by prokaryotes³⁸. The observed prevalence of genes encoding siderophores, growth-promoting hormones, quorum sensing and vitamins reveal that the prokaryotic populations responding to phytoplankton–DOM treatments were considerably enriched in functions that can mediate mutualistic interactions with phytoplankton cells. Our results therefore suggest that chemotaxis has an initial filtering role in the establishment of these important marine symbioses.

The prokaryotic communities exhibiting chemotaxis to each of the ten phytoplankton DOM treatments displayed significantly different functional profiles to one another (PERMANOVA, $P<0.05$; Supplementary

Table 7), indicating functional partitioning of the microbial assemblages responding to different simulated phycospheres. Among the microbial communities exhibiting chemotaxis towards phytoplankton DOM, there was a significant enrichment in a suite of genes involved in the metabolism of phytoplankton-derived compounds¹⁸, such as the osmolyte dimethylsulfoniopropionate, the sulfonate 2,3-dihydroxypropane-1-sulfonate and the polyamine putrescine (*F*-tests, $P < 0.05$; Extended Data Fig. 7, Supplementary Table 8). Genes involved in the uptake of other exogenous substrates (such as sugars, sugar alcohols and amino acids) were also enriched in these treatments (*F*-tests, $P < 0.05$; Extended Data Fig. 7, Supplementary Table 8), although further research is needed to confirm the directionality and substrate specificity of these transporters. Such patterns reveal that marine prokaryotes display chemotactic responses to phytoplankton DOM that are potentially linked to their ability to uptake and metabolize specific DOM components.

Confirmation of the roles of chemoattractants

To further identify specific chemical compounds underpinning chemotactic responses, we examined correlations in the relative abundance of each chemical identified in a phytoplankton-derived DOM with the relative abundance of each responding prokaryotic taxon in the corresponding ISCA wells. We identified 131 significant positive correlations (Pearson's correlation, $P < 0.05$; Fig. 4a) linked to 46 compounds, some of which are known to have important roles in the metabolic relationships between bacteria and phytoplankton, such as xylose, putrescine and glutamate³⁹. Some prokaryotic taxa were significantly correlated to more than one compound. Among them, members of the *Agarivorans* genus (Celerinatantimonadaceae) exhibited the strongest correlations with ethanalamine, putrescine, glycerol and erythritol, whereas *Photobacterium* (Vibrionaceae) were highly correlated with gluconate, digalactosylglycerol, galactose and succinate. In addition, members of the *Maribacter* (Flavobacteriaceae) and Poseidoniales (Marine Group II), the most abundant archaeal group in the surface ocean⁴⁰, were highly correlated with xylitol, citric acid, proline, ornithine, lysine, 3-aminopiperidin-2-one and three unknown compounds.

To validate the importance of these specific compounds in driving chemotactic behaviour, we performed additional laboratory-based chemotaxis assays, in which the chemotactic responses of the marine isolates *A. albus*, *Photobacterium* sp. and *M. dokdonensis* were measured towards the compounds with which they were significantly correlated. These experiments revealed that 18 out of 22 compounds tested (81.8%) significantly attracted these isolates (ANOVA, $P < 0.05$; Fig. 4b). Some compounds not previously implicated in phytoplankton-prokaryote interactions were identified as chemoattractants, such as the sugar alcohol erythritol (mostly found in the DOM from the green algae *Dunaliella*) or 3-aminopiperidin-2-one (which was particularly abundant in *Phaeodactylum*-derived DOM; Fig. 4b). Our results therefore strongly suggest that these compounds constitute previously unrecognized chemotactic cues and chemical currencies in the marine food web. To assess whether these compounds are metabolized by responding bacteria, in addition to acting as chemoattractants, we performed growth assays on each of the 18 identified chemoattractants. These experiments showed that 12 of these 18 compounds (66.6%) were also used by the isolates to support growth (Fig. 4b, Extended Data Fig. 8), revealing a direct link between chemotactic behaviour and the ability of these microorganisms to metabolize specific molecules. The remaining 6 compounds (33.3%) therefore may act as non-metabolizable signals that are used solely to locate specific microenvironments, illustrating the different ecological functions underpinning chemotaxis.

Conclusion

Marine microbial processes are generally examined at the community level across large spatiotemporal scales. Here we used *in situ*

microfluidics to interrogate microbial behaviours at the microscale. Our sampling strategy captured seasonal changes in the extent of chemotaxis at a single site, but we acknowledge that spatial variability (that is, across different environments and depths) in chemotactic responses is also likely to occur according to local physicochemical conditions (including microscale gradients in other signals such as viscosity, pH or dissolved gases), and that this warrants future research. Furthermore, the chemotactic behaviour observed here is unlikely to be restricted to prokaryotes, with some marine protists also being capable of foraging responses to microscale chemical hotspots⁴¹, but longer deployment times of the ISCA would be required to attract a sufficient number of eukaryotic cells.

Metabolic responses of marine prokaryotes to microscale chemical heterogeneity in the water column have been predicted to generate activity hotspots that influence all major pathways of elemental flux in the ocean^{1,12}. Our *in situ* experiments demonstrate that DOM derived from phytoplankton induce specific chemotactic responses across a broad range of prokaryotes in natural marine assemblages. We identified generalist and specialist chemotactic responses by diverse groups of bacteria and archaea, the molecules involved in these responses, and showed that the prokaryotic taxa attracted to phytoplankton DOM were enriched in functions conducive to symbiotic relationships. Together, these observations provide *in situ* evidence that chemotactic behaviour promotes the selective recruitment of specific marine prokaryotes and leads to microscale partitioning of biogeochemical transformation processes in the ocean. By revealing this rich tapestry of microbial interactions through *in situ* microscale observations, these results provide the basis for quantifying the role of chemotaxis in accessing microscale hotspots in marine systems and an opportunity to scale up the impact of these processes on the ocean's biogeochemistry.

Online content

Any methods, additional references, Nature Research reporting summaries, source data, extended data, supplementary information, acknowledgements, peer review information; details of author contributions and competing interests; and statements of data and code availability are available at <https://doi.org/10.1038/s41586-022-04614-3>.

1. Azam, F. & Malfatti, F. Microbial structuring of marine ecosystems. *Nat. Rev. Microbiol.* **5**, 782–791 (2007).
2. Blackburn, N., Fenchel, T. & Mitchell, J. Microscale nutrient patches in planktonic habitats shown by chemotactic bacteria. *Science* **282**, 2254–2256 (1998).
3. Stocker, R. Marine microbes see a sea of gradients. *Science* **338**, 628 (2012).
4. Levin, S. A. The problem of pattern and scale in ecology. *Ecology* **73**, 1943–1967 (1992).
5. Azam, F. Microbial control of oceanic carbon flux: the plot thickens. *Science* **280**, 694–696 (1998).
6. Strom, S. L. Microbial ecology of ocean biogeochemistry: a community perspective. *Science* **320**, 1043–1045 (2008).
7. Sarmento, H. & Gasol, J. M. Use of phytoplankton-derived dissolved organic carbon by different types of bacterioplankton. *Env. Microbiol.* **14**, 2348–2360 (2012).
8. Grossart, H.-P., Riemann, L. & Azam, F. Bacterial motility in the sea and its ecological implications. *Aquat. Microb. Ecol.* **25**, 247–258 (2001).
9. Brumley, D. R. et al. Bacteria push the limits of chemotactic precision to navigate dynamic chemical gradients. *Proc. Natl Acad. Sci. USA* **116**, 10792–10797 (2019).
10. Fenchel, T. Eppur si muove: many water column bacteria are motile. *Aquat. Microb. Ecol.* **24**, 197–201 (2001).
11. Son, K., Menolascina, F. & Stocker, R. Speed-dependent chemotactic precision in marine bacteria. *Proc. Natl Acad. Sci. USA* **113**, 8624–8629 (2016).
12. Fenchel, T. Microbial behavior in a heterogeneous world. *Science* **296**, 1068–1071 (2002).
13. Kiørboe, T. & Jackson, G. A. Marine snow, organic solute plumes, and optimal chemosensory behavior of bacteria. *Limnol. Oceanogr.* **46**, 1309–1318 (2001).
14. Lambert, B. S., Fernandez, V. I. & Stocker, R. Motility drives bacterial encounter with particles responsible for carbon export throughout the ocean. *Limnol. Oceanogr. Lett.* **4**, 113–118 (2019).
15. Wadhams, G. H. & Armitage, J. P. Making sense of it all: bacterial chemotaxis. *Nat. Rev. Mol. Cell. Biol.* **5**, 1024–1037 (2004).
16. Stocker, R., Seymour, J. R., Samadani, A., Hunt, D. E. & Polz, M. F. Rapid chemotactic response enables marine bacteria to exploit ephemeral microscale nutrient patches. *Proc. Natl Acad. Sci. USA* **105**, 4209–4214 (2008).
17. Raina, J.-B., Fernandez, V., Lambert, B., Stocker, R. & Seymour, J. R. The role of microbial motility and chemotaxis in symbiosis. *Nat. Rev. Microbiol.* **17**, 284–294 (2019).

18. Seymour, J. R., Amin, S. A., Raina, J.-B. & Stocker, R. Zooming in on the phycosphere: the ecological interface for phytoplankton–bacteria relationships. *Nat. Microbiol.* **2**, 17065 (2017).
19. Bell, W. & Mitchell, R. Chemotactic and growth responses of marine bacteria to algal extracellular products. *Biol. Bull.* **143**, 265–277 (1972).
20. Smriga, S., Fernandez, V. I., Mitchell, J. G. & Stocker, R. Chemotaxis toward phytoplankton drives organic matter partitioning among marine bacteria. *Proc. Natl Acad. Sci. USA* **113**, 1576–1581 (2016).
21. Amin, S. A. et al. Interaction and signalling between a cosmopolitan phytoplankton and associated bacteria. *Nature* **522**, 98–101 (2015).
22. Lambert, B. S. et al. A microfluidics-based *in situ* chemotaxis assay to study the behaviour of aquatic microbial communities. *Nat. Microbiol.* **2**, 1344–1349 (2017).
23. Larsen, M. H., Blackburn, N., Larsen, J. L. & Olsen, J. E. Influences of temperature, salinity and starvation on the motility and chemotactic response of *Vibrio anguillarum*. *Microbiology* **150**, 1283–1290 (2004).
24. Rinke, C. et al. Validation of picogram- and femtogram-input DNA libraries for microscale metagenomics. *PeerJ* **4**, e2486 (2016).
25. Becker, J. et al. Closely related phytoplankton species produce similar suites of dissolved organic matter. *Front. Microbiol.* **5**, 111 (2014).
26. Vrapsir, J. M. & Butler, A. Chemistry of marine ligands and siderophores. *Annu. Rev. Mar. Sci.* **1**, 43–63 (2009).
27. Tagliabue, A. et al. The integral role of iron in ocean biogeochemistry. *Nature* **543**, 51–59 (2017).
28. Hopkinson, B. M. & Morel, F. M. M. The role of siderophores in iron acquisition by photosynthetic marine microorganisms. *BioMetals* **22**, 659–669 (2009).
29. Amin, S. A. et al. Photolysis of iron–siderophore chelates promotes bacterial–algal mutualism. *Proc. Natl Acad. Sci. USA* **106**, 17071–17076 (2009).
30. Croft, M. T., Lawrence, A. D., Raux-Deery, E., Warren, M. J. & Smith, A. G. Algae acquire vitamin B12 through a symbiotic relationship with bacteria. *Nature* **438**, 90–93 (2005).
31. Hellawell, K. E. The roles of B vitamins in phytoplankton nutrition: new perspectives and prospects. *New Phytol.* **216**, 62–68 (2017).
32. Berg, G. Plant–microbe interactions promoting plant growth and health: perspectives for controlled use of microorganisms in agriculture. *Appl. Microbiol. Biotechnol.* **84**, 11–18 (2009).
33. Christie, P. J., Whitaker, N. & González-Rivera, C. Mechanism and structure of the bacterial type IV secretion systems. *Biochim. Biophys. Acta* **1843**, 1578–1591 (2014).
34. Preston, G. M. Metropolitan microbes: type III secretion in multihost symbionts. *Cell Host Microbe* **2**, 291–294 (2007).
35. Deakin, W. J. & Broughton, W. J. Symbiotic use of pathogenic strategies: rhizobial protein secretion systems. *Nat. Rev. Microbiol.* **7**, 312–320 (2009).
36. Luo, H. & Moran, M. A. Evolutionary ecology of the marine Roseobacter clade. *Microbiol. Mol. Biol. Rev.* **78**, 573–587 (2014).
37. Rolland, J. L., Stien, D., Sanchez-Ferandin, S. & Lami, R. Quorum sensing and quorum quenching in the phycosphere of phytoplankton: a case of chemical interactions in ecology. *J. Chem. Ecol.* **42**, 1201–1211 (2016).
38. Fei, C. et al. Quorum sensing regulates ‘swim-or-stick’ lifestyle in the phycosphere. *Environ. Microbiol.* **22**, 4761–4778 (2020).
39. Landa, M., Burns, A. S., Roth, S. J. & Moran, M. A. Bacterial transcriptome remodeling during sequential co-culture with a marine dinoflagellate and diatom. *ISME J.* **11**, 2677 (2017).
40. Rinke, C. et al. A phylogenomic and ecological analysis of the globally abundant Marine Group II archaea (Ca. *Poseidoniales* ord. nov.). *ISME J.* **13**, 663–675 (2019).
41. Fenchel, T. & Blackburn, N. Motile chemosensory behaviour of phagotrophic protists: mechanisms for and efficiency in congregating at food patches. *Protist* **150**, 325–336 (1999).

Publisher's note Springer Nature remains neutral with regard to jurisdictional claims in published maps and institutional affiliations.

© The Author(s), under exclusive licence to Springer Nature Limited 2022

Methods

Phytoplankton cultures

Fourteen phytoplankton cultures were selected, each based on their cosmopolitan distribution, occurrence in the coastal waters of Sydney, Australia (Supplementary Table 1), and taxonomic diversity. Cultures were grown at their optimal light, temperature and nutrient conditions (see Supplementary Table 10 for the full list of phytoplankton taxa and culture conditions). The growth dynamic of each phytoplankton culture was predetermined by conducting growth curves using flow cytometry (see below). To grow cells for chemotaxis assays, four flasks per species containing 250 ml cultures were monitored twice a day for photophysiology parameters (photosynthetic efficiency (F_v/F_M) and chlorophyll) using fast-repetition rate fluorometry (FastOcean MKIII, Chelsea Technologies) coupled to a FastAct laboratory system (Chelsea Technologies). The system was programmed to deliver single turnover saturation of photosystem II from a succession of 100 flashlets (1 μ s pulse with a 2 μ s interval between flashes), followed by a relaxation phase of 40 flashlets (1 μ s pulse with a 50 μ s interval between flashes). A total of 40 sequences were performed per acquisition, with an interval of 150 ms between sequences⁴². Algal cells were collected when their F_v/F_M was at its maximal value and chlorophyll was exponentially increasing (mid-exponential phase).

Metabolomics

Sample preparation. The content of each algal culture flask was split as follows: (1) 70 ml allocated for metabolomics, (2) the remaining 180 ml allocated for ISCA deployments. Samples were centrifuged at low speed (1,500g for 10 min, room temperature), supernatant was removed, and the algal pellet was snap frozen in liquid nitrogen and kept at -80 °C until required. Chemical extractions for metabolomics were carried out as follows: frozen algal pellets were freeze-dried overnight and extracted using 450 μ l HPLC-grade methanol (containing internal standards (ITSD) at a 0.5% final concentration: $^{13}\text{C}_6$ -sorbitol; ^{13}C - ^{15}N -valine, penta-fluorobenzoic acid and 2-aminoanthracene). Samples were mixed briefly, and the extract and cell slurry were transferred into a 2 ml Eppendorf tube. The process was repeated with an extra 450 μ l of HPLC-grade methanol (with ITSD), ensuring that no phytoplankton material remained in the freeze-dried tube. The Eppendorf tubes were mixed by vortexing, then sonicated for 10 min on ice to rupture the cells, before being incubated for 30 min in a thermomixer at 1,000 rpm (room temperature). Tubes were then centrifuged at 13,000 rpm for 10 min (room temperature), and supernatant was transferred into new Eppendorf tubes. The remaining cell debris were resuspended in 900 μ l of 50% HPLC-grade methanol (without ITSD), incubated for 30 min in a thermomixer at 1,000 rpm and then centrifuged at 13,000 rpm for 10 min (room temperature). Supernatants were combined, mixed and centrifuged at 13,000 rpm for 10 min at 4 °C. The final supernatant was transferred into a new tube, dried using a vacuum concentrator (Vacufuge, Eppendorf) and analysed using a metabolomic approach. The same extraction protocol was followed for the samples allocated to ISCA deployments, with the exception that no internal standards were added to the methanol. At the end of the extraction protocol, each extract was aliquoted, dried using a vacuum concentrator and the resulting dry weight was quantified.

Sample derivatization. Dried samples for untargeted analysis were prepared by adding 20 μ l of methoxyamine hydrochloride (30 mg ml⁻¹ in pyridine) followed by shaking at 37 °C for 2 h. Samples were then derivatized with 20 μ l of N,O-bis(trimethylsilyl)trifluoroacetamide with trimethylchlorosilane (BSTFA with 1% TMCS) (Thermo Scientific) for 30 min at 37 °C. The sample was left for 1 h before 1 μ l was injected into the GC column using a hot needle technique. Splitless and split (1:20) injections were done for each sample.

Analytical instrumentation. The GC-MS system used to characterize phytoplankton DOM composition consisted of a Gerstel 2.5.2

autosampler, a 7890A Agilent gas chromatograph and a 5975C Agilent quadrupole mass spectrometer (Agilent). The mass spectrometer was tuned according to the manufacturer's recommendations using tris-(perfluorobutyl)-amine (CF43). GC-MS was performed on a 30 m Agilent J & W VF-SMS column with 0.25 μ m film thickness and 0.25 mm internal diameter with a 10 m Integraguard column. The injection temperature (Inlet) was set at 250 °C, the MS transfer line at 280 °C, the ion source adjusted to 230 °C and the quadrupole at 150 °C. Helium was used as the carrier gas at a flow rate of 1 ml min⁻¹. The analysis of TMS samples was performed under the following temperature program; start at injection 70 °C, a hold for 1 min, followed by a 7 °C min⁻¹ oven temperature ramp to 325 °C and a final 6 min heating at 325 °C. Mass spectra were recorded at 2.66 scans s⁻¹ with an m/z 50-600 scanning range. Both chromatograms and mass spectra were evaluated using the Agilent MassHunter Qualitative and Quantitative Analysis version B.08.00 software and AMDIS software. Mass spectra of eluting TMS compounds were identified using the commercial mass spectra library NIST (<http://www.nist.gov>), the public domain mass spectra library of Max-Planck-Institute for Plant Physiology, Golm, Germany (<http://csbdb.mpimp-golm.mpg.de/csbdb/dbma/msri.html>) and the in-house Metabolomics Australia mass spectral library (containing chemical reference standards). This approach is classified as level 1-2 according to the proposed reporting standards by the Metabolomics Standards Initiative⁴³. Resulting area responses were normalized to the ITSD $^{13}\text{C}_6$ Sorbitol area response and to the dry weight of the extracts. The raw data files were deposited in MetaboLights (accession number: MTBLS1980).

Data analysis. Metabolomic data were analysed using MetaboAnalyst 4.0^{44,45}. Normalized data were log-transformed (glog), mean-centred and displayed as a heat map and principal component analysis (PCA) in Figure 1c and Figure S3. To determine if statistical differences existed between phytoplankton-derived DOM treatments, a Bray-Curtis similarity matrix was generated on the normalized data. A permutational multivariate analyses of variance (PERMANOVA) was carried out using PRIMER (v6), with 999 unrestricted permutations.

ISCA design and assembly

ISCA moulds were 3D-printed out of the polymer VeroGrey on an Objet30 3D printer (Stratasys), using previously described designs and protocols^{22,46}. Each ISCA consisted of an array of 5 × 5 wells, linked to the outside environment by an 800- μm -diameter port, emitting chemical gradients that are analogous to those around large phytoplankton cells, nutrient patches, or marine aggregates^{20,22}. Each mould was filled with 25 g of polydimethylsiloxane (PDMS) (10:1 PDMS base to curing agent, wt/wt; Sylgard 184, Dow Corning). Curing was carried out overnight at 40 °C. The cured PDMS slab (95 mm × 65 mm × 4.6 mm) was cut using a razor blade and carefully peeled from the mould. The PDMS blocks were inspected and any port obstructions were cleared using a biopsy punch (ProSciTech). Finally, the devices were UV-sterilized and plasma-bonded to sterile glass microscope slides (100 mm × 76 mm × 1 mm, VWR) by exposing both to oxygen plasma for 5 min using a plasma cleaner/sterilizer (Harrick Scientific). Following bonding, the ISCA was heated at 90 °C for 10 min to accelerate the formation of covalent bonds and then stored at room temperature, covered with a protective film, until use.

Field deployments

Field deployments were carried out between April 2016 and March 2018 at Clovelly Beach (33.91°S, 151.26°E), a coastal location near Sydney, on the eastern coast of Australia. We used seawater freshly collected from the field site and applied an ultra-filtration protocol to ensure the complete removal of microbial cells^{22,46}. This ultrafiltered seawater acted as a control in the ISCA and was also used to resuspend all dried phytoplankton-derived DOM treatments, maintaining the same water

Article

chemistry as the surrounding seawater. Specifically, 60 mL were collected from the field site and filtered first through a 0.2 µm Millex FG (Merck Millipore); followed by two successive filtrations through a 0.22 µm Sterivex filter (Merk Millipore), and finally through a 0.02 µm Anotop filter (Whatman). Four replicate samples (80 µl) of this ultrafiltered seawater were fixed in 2% glutaraldehyde (prefiltered at 0.2 µm) for subsequent flow cytometry analysis, which confirmed the effectiveness of this filtration protocol in removing bacterial cells from seawater. In addition, ultrafiltered seawater samples were collected as blanks for subsequent DNA extractions and sequencing.

We used DOM derived from 10–12 different phytoplankton as chemotaxants in each deployment. Each treatment was resuspended with ultrafiltered seawater to a final concentration of 1 mg ml⁻¹. Notably, chemical concentrations decay exponentially with distance away from the ISCA port, meaning that concentrations experienced by prokaryotes in the surrounding seawater will be substantially lower (see supplementary note 2 in ref.²²). Treatments (filtered seawater and each 10 phytoplankton DOM) were randomly allocated to an ISCA row (consisting of 5 wells). All wells in a row contained the same treatment, with each treatment replicated on four discrete ISCAs, which were deployed in parallel to act as biological replicates²². As previously described, each ISCA was secured inside a transparent flow-damping enclosure, which prevents the disruption or interaction of the chemical microplumes emanating from the ports²². The enclosure was completely sealed in situ and deployed at 1 m depth for 1 h.

Upon retrieval, the contents of ISCA wells were then collected using 1 ml syringes and 27G needles (Terumo). For each ISCA, the liquid from each row (five wells containing the same treatment) was pooled to increase the volume collected per sample for downstream analyses. The total volume of each pooled sample recovered was approximately 500 µl, of which 100 µl were fixed with filtered glutaraldehyde (2% final concentration) for flow cytometry analysis (conducted the same day) and 400 µl were snap-frozen immediately in liquid nitrogen for subsequent DNA extraction and sequencing. In addition to the ISCA samples ($n = 4$), bulk seawater samples (500 µl, $n = 4$) were also collected for both flow cytometry and DNA sequencing.

This sampling strategy was used to capture seasonal changes in the extent of chemotaxis at a single site, but we acknowledge that spatial (that is, inter-environment) variability in chemotaxis strength is also likely to occur according to local physicochemical conditions (including microscale gradients in other signals such as viscosity, pH or dissolved gases), and that this warrants future research.

Environmental data

Water temperature, salinity, pH and oxygen levels were recorded during the ISCA deployments using a multiprobe meter (WTW). Seawater samples were collected in triplicate for inorganic nutrient analyses: 50 ml per sample were filtered through 0.45 µm pore size and frozen at -20 °C until analysis. Nitrite (NO₂⁻), nitrate (NO₃⁻), ammonia (NH₃) and phosphate (PO₄³⁻) were then quantified on an Aquakem analyser (Thermo Scientific) using standard colorimetric techniques (APHA NO₂⁻B, APHA 4500-NH₃F, APHA 4500 PE, practical quantification limit: 0.005 mg l⁻¹). Seawater samples were also collected in triplicate for chlorophyll concentrations, 200 ml per sample were filtered through 0.7 µm glass fibre filters (GF/F, Whatman), which were snap-frozen in liquid nitrogen and stored at -80 °C until required. Samples were extracted with ice cold ethanol, cells were lysed by sonication into an ice bath (10 min), and incubated overnight at -20 °C. The next day samples were vortexed, centrifuged (4 °C, 5 min, 1,000g) and absorption was immediately recorded at 629, 649, 665 and 696 nm using a FLU-Ostar Omega microplate reader (BMG Labtech). Chlorophyll *a* content was calculated following established protocols⁴⁷. All environmental metadata are reported in Supplementary Table 2. To ensure that the low-volume bulk seawater samples (500 µl, $n = 4$) were representative of the bacterial communities at the site, triplicate 10 l samples were

collected simultaneously, transported to the laboratory, and filtered upon arrival through 0.2 µm Sterivex cartridges (Millipore). All cartridges were sealed with parafilm and were preserved at -80 °C for further processing.

Flow cytometry

Samples for flow cytometry were transferred into sterile Titertube micro test tubes (Bio-Rad), stained with SYBR Green (1:10,000 final dilution; ThermoFisher), incubated for 15 min in the dark and analysed on a CytoFLEX S flow cytometer, using CytExpert version 2.4 (Beckman Coulter) with filtered MilliQ water as sheath fluid. For each sample, forward scatter (FSC), side scatter (SSC), and green (SYBR) fluorescence were recorded. The samples were analysed at a flow rate of 25 µl min⁻¹. Microbial populations were characterized according to SSC and SYBR Green fluorescence⁴⁸ (Fig. S1) and cell abundances were calculated by running a standardized volume of sample (50 µl). To quantify the strength of chemotaxis, the chemotactic index I_c was calculated by dividing the number of cells present in the phytoplankton-DOM treatment by the average number of cells present in the filtered seawater control²².

DNA extraction

DNA extraction from all ISCA samples was performed under a UV cleaner hood (UVC/T-M-AR, Biosan) using a recently developed physical lysis extraction designed for microvolume samples⁴⁹. All tubes and reagents (except ethanol and magnetic beads) were UV-sterilized for 1 h in a UV-crosslinker (CL-1000 Ultraviolet Crosslinker, UVP). In brief, 300 µl of sample were mixed with 162.5 µl of lysis buffer (made by mixing 700 µl of KOH (0.0215 g ml⁻¹), 430 µl of DTT (0.008 g ml⁻¹) and 520 µl of UV-treated Ultrapure water; pH12) and incubated for 10 min at room temperature. Samples were then frozen at -80 °C for 15 min, followed by an incubation on a heat block at 55 °C for 5 min. Following this freeze-thaw cycle, 162.5 µl of STOP buffer (Tris-HCl 0.4 g ml⁻¹; pH5) were added and mixed to bring the pH of the solution to 8. AMPure beads (1,250 µl; Beckman Coulter) were added to each sample to capture the DNA, then mixed and incubated for 15 min at room temperature, the sample tubes were then placed on a magnetic stand for 10 min. The supernatant was removed and the beads were washed twice with 80% ethanol (molecular biology grade), all residual ethanol was removed and the beads were left to air-dry for 15 min. Tubes were removed from the magnetic stand and 20 µl of elution buffer (10 mM Tris-HCl) were added, mixed by pipetting and the solution incubated for 5 min at room temperature. Finally, tubes were placed on a magnetic stand and 18 µl of bead-free liquid was transferred to a new tube. Samples were stored at -20 °C until library preparation.

Library preparation and sequencing

Libraries for shotgun metagenomic sequencing were prepared using the Nextera XT DNA Sample Preparation Kit (Illumina) following a previously described protocol designed for generating low-input DNA libraries²⁴, and ISCA treatments were all processed the same way. All libraries were sequenced on the Illumina NextSeq 500 platform 2 × with 150 bp High Output v.2 run chemistry, with the analysis including a total of 69 samples: 44 ISCA samples, 7 bulk seawater samples and 18 controls (2 mock communities, 3 DNA extraction controls, 2 library prep controls, and 11 undeployed ISCA controls). These additional controls were used to identify and remove potential reagent contaminants. Libraries were pooled on an indexed shared sequencing run, resulting in ~3 Gbp per sample. The raw fastq read files were deposited in Sequence Read Archive (SRA) (accession number: PRJNA639602).

Metagenomics

Quality control of the reads. Reads were processed using Trimmomatic v0.36⁵⁰ to remove adapters, filter leading or trailing bases with a quality score <3, clip reads when the average 4-base window had a

quality score <15, and discard reads <50 bp in length after applying the previous QC steps. Read pairs passing QC ($87.6\% \pm 0.42$ on average, excluding controls), ranging from 11,082,294 to 35,206,174 reads, were further processed to remove potential human contamination or contamination from the phytoplankton species used to produce DOM. Specifically, paired reads were mapped to reference genomes or available transcriptomic data (Supplementary Table 11) using the MEM mapping method of BWA v 0.7.12-r1039⁵¹ and pairs were removed from further consideration if either read had a percent identity $\geq 95\%$ and percent alignment length $\geq 95\%$ to any reference sequence. QC results are available in Supplementary Table 12.

Taxonomic profiles. The 16S rRNA gene-based taxonomic profiles of the samples were generated with GraftM v0.11.1⁵² using the 7.05.2013_08_greengenes_97_otus.gpkg reference package. GraftM identifies reads encoding 16S rRNA genes using hidden Markov models and assigns taxonomic classifications to these reads by placing them into an annotated reference tree. The GraftM output was manually curated to removed reads classified as mitochondrial or chloroplast sequences. Relative abundances were calculated in the R software environment (<https://www.r-project.org>) and all taxa present in blanks at $>0.5\%$ relative abundance were removed prior to subsequent analyses. Surprisingly, members of Desulfobacteraceae, a bacterial family thought to be primarily anaerobic, were present in some ISCA treatments. As sequences originating from this family were completely absent from our blank samples (un-deployed filtered seawater and DNA extraction blanks), we are confident that they are not a contaminant. Members of the Desulfobacteraceae are known to be highly motile⁵³, and have therefore the capacity to migrate into the ISCA wells. In addition, recent evidence has shown that prokaryotes that are thought to be primarily anaerobic can inhabit oxygenated pelagic water columns, potentially within anoxic microenvironments associated with particles^{54,55}. Note: the taxonomy presented in the main text is compatible with the Genome Taxonomy Database (GTDB)⁵⁶ (release O6-RS202).

Functional profiles. A reference database was constructed from all UniRef100⁵⁷ proteins available on 6 March, 2018 which had a KEGG Orthology (KO) annotation in the KEGG database⁵⁸. Quality-controlled reads were compared with this reference database using the BLASTX option of DIAMOND v0.9.22⁵⁹. A read was assigned to a UniRef protein if the top hit had an E-value $<10^{-3}$, a percent identity $>30\%$, an alignment covering $>70\%$ of the read, and the UniRef100 protein was annotated as being bacterial or archaeal. Otherwise, the read was considered unclassified. Assigned reads were mapped to KO IDs using UniProt ID mapping files. In a small number of cases, a read was assigned to multiple KOs ($<0.2\%$ across all ISCA samples). Hits to each KO were summed across all assigned reads to produce a KO count table for each sample.

Statistical analysis. Normalized sequence counts were generated using variance-stabilizing normalization on the raw counts⁶⁰, using the R package metagenomeSeq version 1.26.3 (functions cumNormStat-Fast and cumNorm)⁶⁰. This normalization method corrects for biases associated with uneven sequencing depth^{60,61}. We then employed a zero-inflated Gaussian mixture model⁶⁰ to determine if the abundance of prokaryotic taxa and functional genes were significantly different between treatments. To determine if statistical differences existed at the taxonomic and functional levels between treatments, Bray–Curtis similarity matrices were generated on the relative abundances of normalized reads. PERMANOVA were carried out using PRIMER (v6), with 999 unrestricted permutations.

Phytoplankton-derived metabolomes were correlated with taxonomic profiles (all data were log transformed) using Pearson's correlation with adjusted P values (using the Holm–Bonferroni method). Data handling and production of graphics was performed using the following R packages: tidyR, dplyr, tibble, pheatmap, psych, ggplot2, metagenomeSeq,

metaboanalyst and mixomics. Networks were produced using the R package tidyverse and edited using Gephi. All analysis scripts are available on GitHub (<https://github.com/JB-Raina-codes/ISCA-paper>).

Laboratory-based chemotaxis assays

Cultured strains of the *Agarivorans*, *Photobacterium* and *Maribacter* genera, isolated from phytoplankton species used in this experiment (*Maribacter*: *Thalassiosira pseudonana*; *Photobacterium*: *Thalassiosira pseudonana*; *Agarivorans*: *Chaetoceros muelleri*) were used in subsequent laboratory assays. Bacterial strains were grown for 4 h in 1% Marine Broth (BD Difco), washed with artificial seawater and resuspended in artificial seawater at a concentration of 10^6 cells ml⁻¹. The compounds tested were added to four ISCA replicates ($n = 4$) at a concentration of 1 mM and incubated for 1 h in individual trays. Chemo-tactic cells in each treatment were enumerated by flow cytometry, as previously described. Note: digalactosyldiacylglycerol, the acylated form of digalactosylglycerol, was tested for chemotaxis due to unavailability of a commercial digalactosylglycerol standard. The 16S rRNA gene sequences of the three isolates were deposited in GenBank (accession numbers: MT826233-MT826234 and MZ373175).

Metabolism of chemoattractants

Each compound that was identified as a chemoattractant in the previous set of experiments was also individually tested for its potential to support the growth of the isolates. Bacterial strains were grown overnight in 1% Marine Broth (BD Difco), supplemented with 0.2% casamino acids, washed with artificial seawater and inoculated at a concentration of 10^6 cells per ml into a minimal medium consisting of: artificial seawater⁶² supplemented with 0.2% casamino acids, and 1 mM of chemoattractant ($n = 4$ for each chemoattractant). Bacterial growth was monitored over two days using optical density (OD₆₀₀; two of the bacterial strains (*Agarivorans* and *Maribacter*) formed aggregates at high densities and their density could not be accurately quantified using flow cytometry) and was compared against controls containing only 0.2% casamino acids.

Control tests for ISCA deployment times

To ensure that the *in situ* incubation length (1 h) did not elicit prokaryotic growth in the ISCA wells, which could conceivably lead to increases in cell number (affecting I_c levels) and shifts in prokaryote community composition, we carried out control incubations of the bulk seawater from the Clovelly Beach field site with the 10 phytoplankton-derived DOM used in the ISCA experiments. To mimic the conditions occurring during the ISCA experiments, samples were added to ISCA wells and incubated at 23 °C (same as *in situ* conditions). Samples were taken before incubation (T_0), after one hour (T_1) and after five hours (T_5) in the ISCA wells ($n = 3$). Samples were then divided as previously described and either: (1) fixed with filtered glutaraldehyde (2% final concentration) to enumerate cells via flow cytometry analysis (conducted the same day, same method as above); or (2) snap-frozen immediately in liquid nitrogen for subsequent DNA extraction (same method as above).

To characterize bacterial community composition at each time-point of the incubation, the 27F and 519R primers⁶³, which specifically target the V1-V3 region of the bacterial 16S rRNA gene, were used for PCR amplification of extracted DNA. The PCR reactions included 2.5 µmol of each deoxyribonucleotide triphosphate (Bioline), 6 µl of template, 1 µl of UltraPure Bovine Serum Albumin (Thermo Fisher), 0.25 µl of Velocity DNA polymerase and 5 × PCR buffer (Bioline), 10 pmol of each primer (resuspended in UV-sterilized water) with the following adaptors: 5'-TCGTCGGCAGCGTCAGATGTGTATAAGAGACAG-27F-3'; and 5'-GCTCTCGTGGCTCGGAGATGTGTATAAGAGACAG-519R-3'). The reaction conditions were as follow: 98 °C for 2 min; followed by 30 cycles of 98 °C for 30 s, 30 s of annealing (46 °C for 3 cycles, 48 °C for 3 cycles and 50 °C for 24 cycles), 72 °C for 30 s; and then a final extension of 72 °C for 10 min. PCR clean-up, indexing and sequencing (on an

Article

Illumina MiSeq ($2 \times 300\text{bp}$) were performed at the Australian Genome Research Facility (AGRF), Australia.

Paired end R1 and R2 reads were processed using the DADA2 pipeline (version 1.22.0)⁶⁴. Reads with any 'N' bases were removed, together with primers using cutadapt. R1 and R2 were trimmed to remove low quality terminal ends (trunc(R1 = 260; R2 = 255)), in order to produce the highest number of merged reads after learning error rate and removing chimera sequences. Amplicon sequence variants (ASVs) were then annotated using SILVA (release 138)⁶⁵, using a 50% probability cut-off. The quality ASV table was secondarily filtered to remove ASVs not annotated to kingdom Bacteria, as well as any annotated as chloroplast or mitochondria. We processed and sequenced 2 extraction blanks and 2 PCR blanks, which revealed that 10 ASVs overlapped between the samples and the blanks. After removing these 10 ASVs from the dataset, the samples were rarefied to 25,000 reads using the vegan package⁶⁶ (rrarefy function). The rarefied reads were then filtered to remove singletons. The raw fastq read files were deposited in Sequence Read Archive (SRA) (accession number: PRJNA707306).

These control tests revealed that the cell densities and community compositions did not change significantly during a one-hour incubation (Extended Data Fig. 9, 10). Therefore, these results confirm that the cell abundances and community profiles observed within the ISCA wells occurred as a result of chemotactic migration, not cell growth.

Identification of phytoplankton taxa at coastal sites

To confirm the presence of the phytoplankton genera used for our chemotaxis assay in coastal water of Sydney, Australia, we used publicly available datasets derived from the Australian Microbiome Initiative (<https://data.bioplatforms.com/organization/about/australian-microbiome>). We focused on three coastal sites (Cobblers Beach, Salmon Haul and Taren Point), raw data were processed through the DADA2 pipeline (version 1.22.0)⁶⁴, annotated using SILVA⁶⁵ (release 138), with a taxonomic assignment to >50% bootstrap level.

Reporting summary

Further information on research design is available in the Nature Research Reporting Summary linked to this paper.

Data availability

The raw metabolome data files were deposited in MetaboLights under accession number MTBLS1980. The raw metagenome fastq files were deposited in the Sequence Read Archive (SRA) under accession number PRJNA639602. The raw amplicon fastq files were deposited in the SRA under accession number PRJNA707306. The 16S rRNA gene sequences of the three isolates were deposited in GenBank under accession numbers: MT826233, MT826234 and MZ373175. Source data are provided with this paper.

Code availability

All custom analysis scripts are available on GitHub (<https://github.com/JB-Raina-codes/ISCA-paper>).

42. Hughes, D. J. et al. Impact of nitrogen availability upon the electron requirement for carbon fixation in Australian coastal phytoplankton communities. **63**, 1891–1910 (2018).
43. Sumner, L. W. et al. Proposed minimum reporting standards for chemical analysis. *Metabolomics* **3**, 211–221 (2007).
44. Chong, J., Wishart, D. S. & Xia, J. Using MetaboAnalyst 4.0 for comprehensive and integrative metabolomics data analysis. *Curr. Protoc. Bioinformatics* **68**, e86 (2019).
45. Xia, J. & Wishart, D. S. Web-based inference of biological patterns, functions and pathways from metabolomic data using MetaboAnalyst. *Nat. Protoc.* **6**, 743–760 (2011).
46. Lambert, B. S. & Raina, J.-B. Fabrication and deployment of the *in situ* chemotaxis assay (ISCA). *protocols.io* <https://doi.org/10.17504/protocols.io.kztx6n> (2019).
47. Ritchie, R. J. Consistent sets of spectrophotometric chlorophyll equations for acetone, methanol and ethanol solvents. *Photosynth. Res.* **89**, 27–41 (2006).
48. Marie, D., Partensky, F., Jacquet, S. & Vaultier, D. Enumeration and cell cycle analysis of natural populations of marine picoplankton by flow cytometry using the nucleic acid stain SYBR Green I. *Appl. Environ. Microbiol.* **63**, 186–193 (1997).
49. Bramucci, A. R. et al. Microvolume DNA extraction methods for microscale amplicon and metagenomic studies. *ISME Commun.* **1**, 79 (2021).
50. Bolger, A. M., Lohse, M. & Usadel, B. Trimmomatic: a flexible trimmer for Illumina sequence data. *Bioinformatics* **30**, 2114–2120 (2014).
51. Li, H. Aligning sequence reads, clone sequences and assembly contigs with BWA-MEM. Preprint at <https://doi.org/10.48550/arXiv.1303.3997> (2013).
52. Boyd, J. A., Woodcroft, B. J. & Tyson, G. W. GraftM: a tool for scalable, phylogenetically informed classification of genes within metagenomes. *Nucleic Acids Res.* **46**, e59 (2018).
53. Kuever, J., Rainey, F. A. & Widdel, F. In *Bergey's Manual of Systematics of Archaea and Bacteria* <https://doi.org/10.1002/9781118960608.obm00084> (2015).
54. Bianchi, D., Weber, T. S., Kiko, R. & Deutscher, C. Global niche of marine anaerobic metabolisms expanded by particle microenvironments. *Nat. Geosci.* **11**, 263–268 (2018).
55. Liu, X. et al. Wide distribution of anaerobic ammonium-oxidizing bacteria in the water column of the South China Sea: implications for their survival strategies. *Divers. Distrib.* **27**, 1893–19003 (2021).
56. Parks, D. H. et al. A standardized bacterial taxonomy based on genome phylogeny substantially revises the tree of life. *Nat. Biotechnol.* **36**, 996–1004 (2018).
57. Suzek, B. E., Huang, H., McGarvey, P., Mazumder, R. & Wu, C. H. UniRef: comprehensive and non-redundant UniProt reference clusters. *Bioinformatics* **23**, 1282–1288 (2007).
58. Kanehisa, M. & Goto, S. KEGG: Kyoto Encyclopedia of Genes and Genomes. *Nucleic Acids Res.* **28**, 27–30 (2000).
59. Buchfink, B., Xie, C. & Huson, D. H. Fast and sensitive protein alignment using DIAMOND. *Nat. Methods* **12**, 59 (2014).
60. Paulson, J. N., Stine, O. C., Bravo, H. C. & Pop, M. Differential abundance analysis for microbial marker-gene surveys. *Nat. Methods* **10**, 1200 (2013).
61. McMurdie, P. J. & Holmes, S. Waste not, want not: why rarefying microbiome data is inadmissible. *PLOS Comput. Biol.* **10**, e1003531 (2014).
62. Berge, J. A., Franklin, D. J. & Harrison, P. J. Evolution of an artificial seawater medium: improvements in enriched seawater, artificial water over the last two decades. *J. Phycol.* **37**, 1138–1145 (2001).
63. Lane, D. In *Nucleic Acid Techniques in Bacterial Systematics* (eds Stackebrandt, E. & Goodfellow, M.) 115–175 (1991).
64. Callahan, B. J. et al. DADA2: high-resolution sample inference from Illumina amplicon data. *Nature Methods* **13**, 581–583 (2016).
65. Quast, C. et al. The SILVA ribosomal RNA gene database project: improved data processing and web-based tools. *Nucleic Acids Res.* **41**, D590–D596 (2012).
66. Oksanen, J. et al. Package 'Vegan' Community Ecology Package Version 2 (2013).
67. Durham, B. P. et al. Sulfonate-based networks between eukaryotic phytoplankton and heterotrophic bacteria in the surface ocean. *Nat. Microbiol.* **4**, 1706–1715 (2019).
68. Durham, B. P. et al. Recognition cascade and metabolite transfer in a marine bacteria-phytoplankton model system. *Environ. Microbiol.* **19**, 3500–3513 (2017).
69. Durham, B. P. et al. Cryptic carbon and sulfur cycling between surface ocean plankton. *Proc. Natl. Acad. Sci. USA* **112**, 453–457 (2015).
70. Landa, M. et al. Sulfur metabolites that facilitate oceanic phytoplankton–bacteria carbon flux. *ISME J.* **13**, 2536–2550 (2019).

Acknowledgements The authors thank G. Gorick for his work on Fig. 1a, L. Bennar, G. Kholi, M. Fabris, N. Le Reun, M. Giardina and D. Hughes for laboratory assistance and E. Botté for her support throughout this project. This work was supported by the Gordon and Betty Moore Foundation through a grant to J.R.S., G.W.T., P.H. and R.S. (GBMF3801) and two Investigator Awards to R.S. (GBMF3783 and GBMF9197; <https://doi.org/10.37807/GBMF9197>), and through Australian Research Council grants DP110103091 to J.R.S., G.W.T. and R.S. and DP180100838 to J.R.S., R.S. and J.-B.R. B.S.L. was supported by the Simons Foundation (Award 594111). G.W.T. was supported by an Australian Research Council Future Fellowship (FT170100070). P.H. was supported by Australian Research Council Laureate Fellowship (FL150100038). C.R. was supported by Australian Research Council Future Fellowship (FT1701000213). J.-B.R. was supported by an Australian Research Council Fellowship (DE160100636).

Author contributions J.-B.R., B.S.L., C.R., R.S., P.H., G.W.T. and J.R.S. designed all the experiments. J.-B.R., C.R., A.B. and N.S. performed all the experiments. J.-B.R., A.L. and H.M. generated and analysed the metabolomic data. J.-B.R., C.R., F.R., B.S.L. and D.H.P. generated and analysed the metagenomic data. J.-B.R., M.O., B.S.L., A.B., V.I.F. and B.S. generated and analysed the amplicon data and performed the network and correlative analyses. J.-B.R., B.S.L., R.S. and J.R.S. wrote the manuscript. All authors edited the manuscript before submission.

Competing interests The authors declare no competing interests.

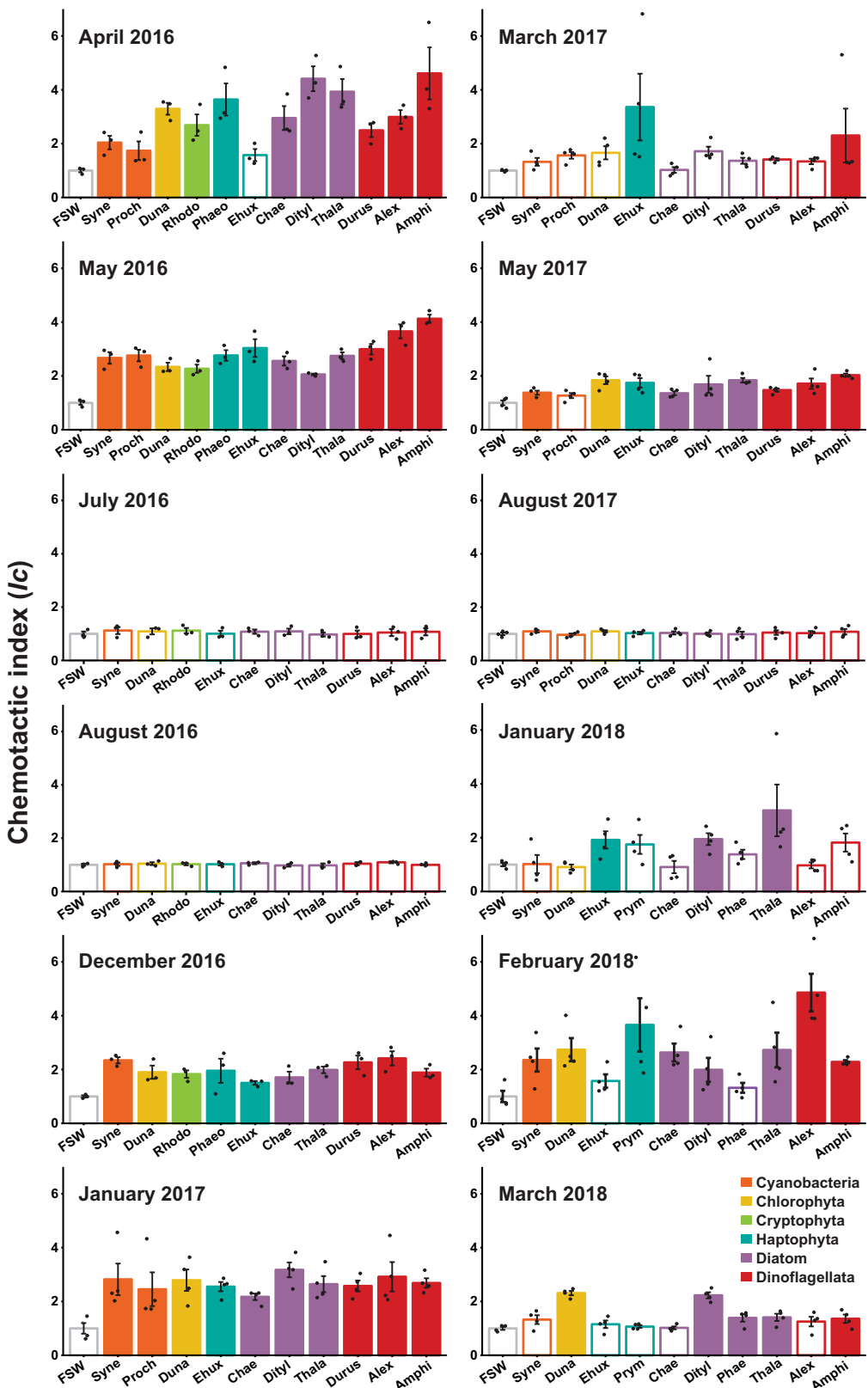
Additional information

Supplementary information The online version contains supplementary material available at <https://doi.org/10.1038/s41586-022-04614-3>.

Correspondence and requests for materials should be addressed to Jean-Baptiste Raina or Justin R. Seymour.

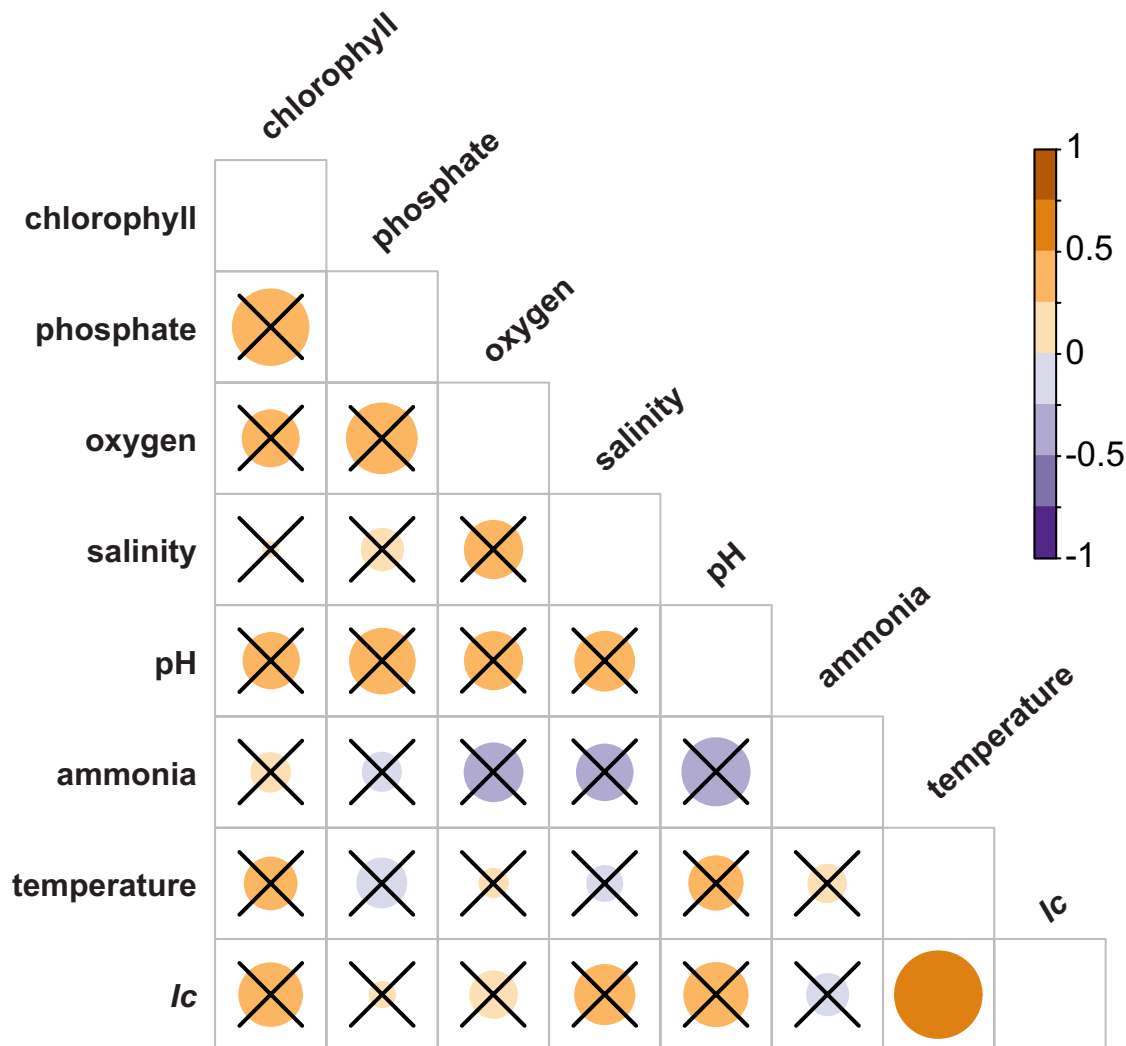
Peer review information *Nature* thanks Hans-Peter Grossart, Karla Heidelberg and the other, anonymous, reviewer(s) for their contribution to the peer review of this work.

Reprints and permissions information is available at <http://www.nature.com/reprints>.



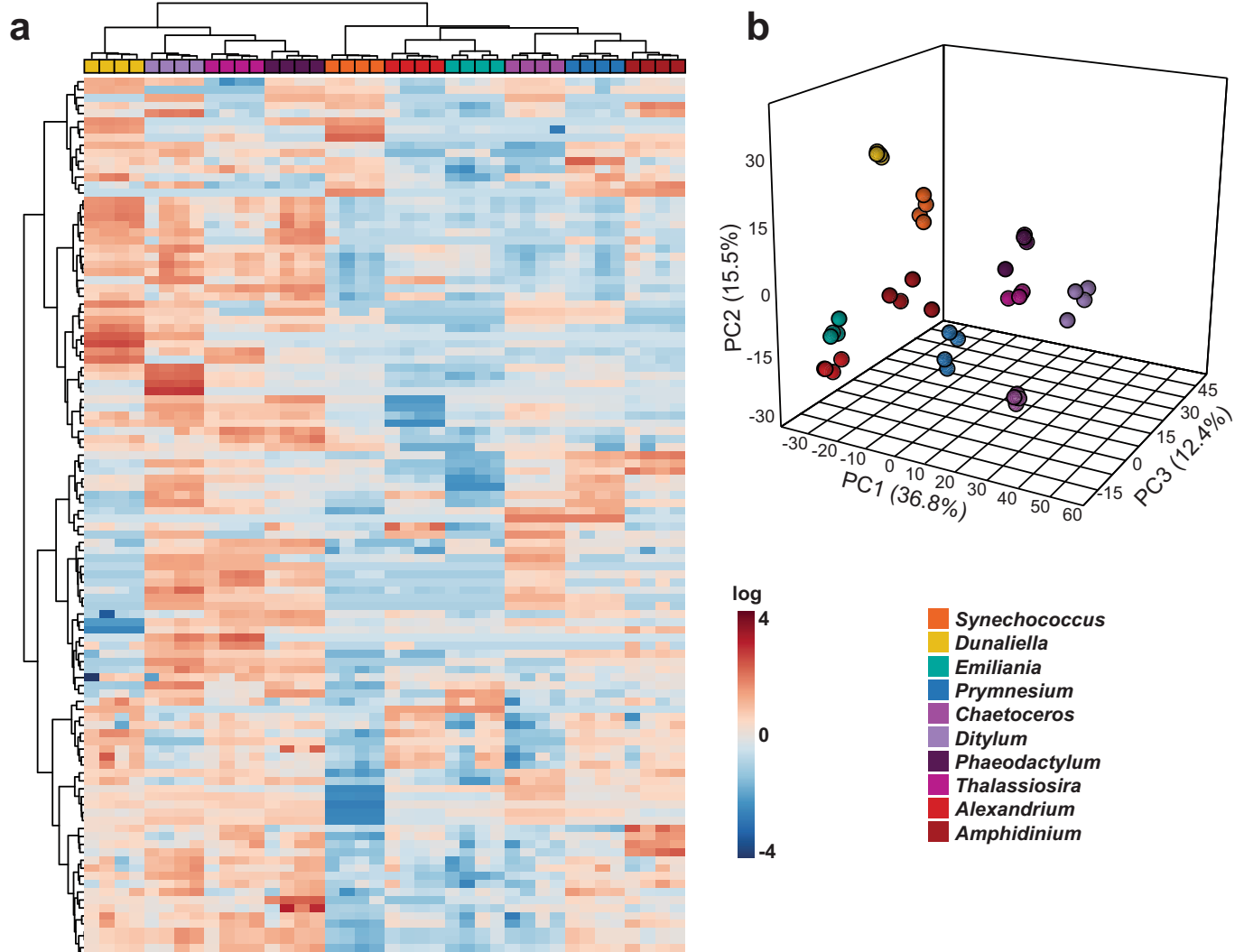
Extended Data Fig. 1 | ISCA deployments through a two years period at Clovelly Beach (33.91°S, 151.26°E). Chemotactic index *lc*, denoting the concentration of cells within ISCA wells, normalized by the mean concentration of cells within wells containing filtered seawater (FSW), after 60 min field deployment. Solid bars are significantly different from wells containing FSW (ANOVA (one-sided), $p < 0.05$, all p -values are reported in Supplementary Table 3). Each treatment was replicated across four different

ISCAs ($n = 4$), except between April and August 2016 ($n = 3$). Data are presented as mean values \pm SEM. FSW: filtered seawater, Syne: *Synechococcus*, Proch: *Prochlorococcus*, Duna: *Dunaliella*, Rhodo: *Rhodomonas*, Phaeo: *Phaeocystis*, Ehux: *Emiliania*, Prym: *Prymnesium*, Chae: *Chaetoceros*, Dityl: *Ditylum*, Phae: *Phaeodactylum*, Thala: *Thalassiosira*, Durus: *Durusdinum*, Alex: *Alexandrium*, Amphi: *Amphidinium*.



Extended Data Fig. 2 | Environmental variables influencing the strength of chemotaxis. (a) Average chemotactic index (I_c) elicited by the phytoplankton-derived DOM for each of the 12 ISCA deployments described in this study at Clovelly Beach (33.91°S, 151.26°E). Error bars: standard errors. (b) Correlogram of the metadata measured during each deployment (the size

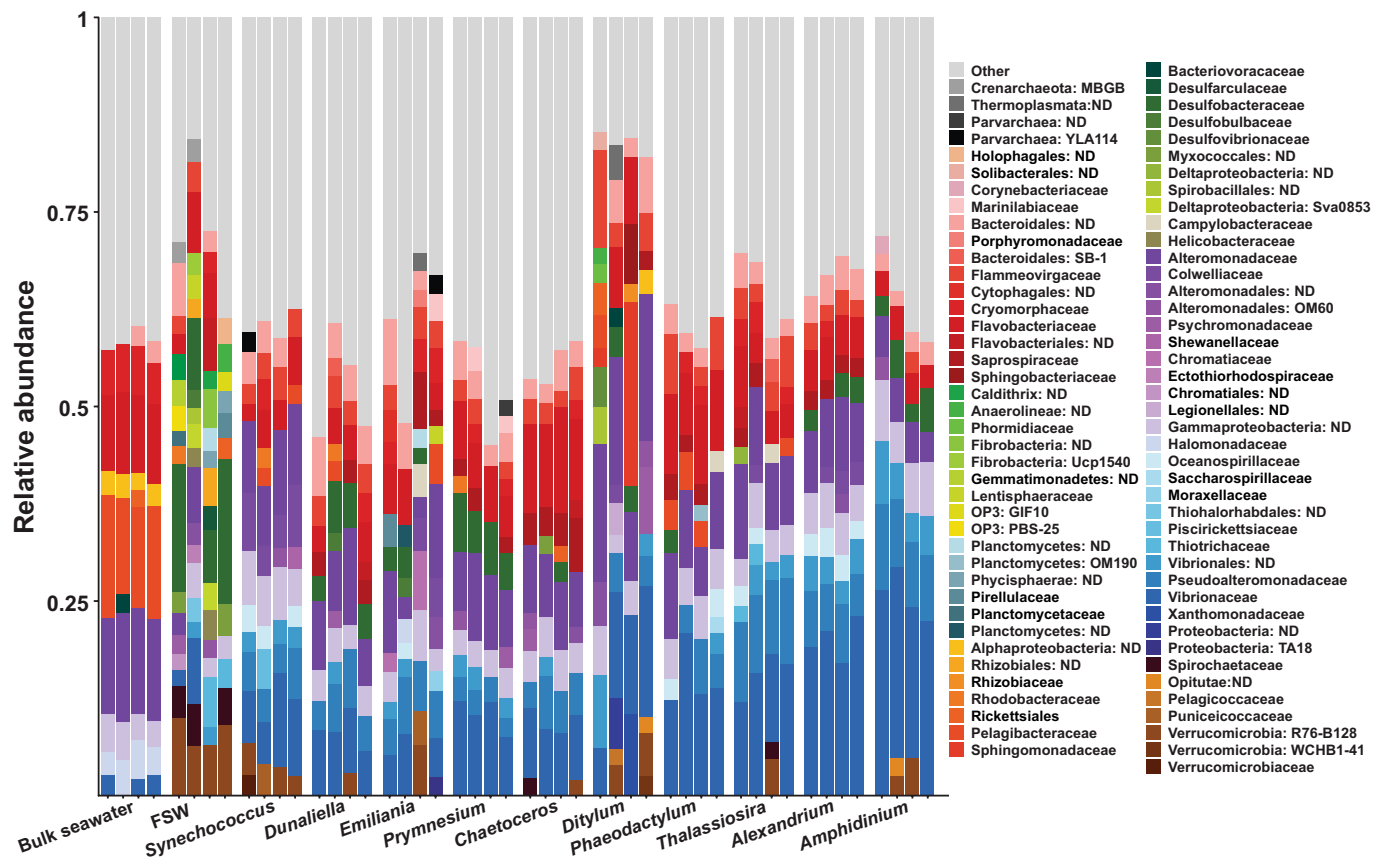
and colour of each bubble is proportional to the strength of the correlation). Only statistically significant correlations are not crossed (Pearson's correlation (two-sided), $p < 0.01$). (c) Significant correlation between chemotactic index and temperature (Pearson's correlation (two-sided), $p < 0.01$).



Extended Data Fig. 3 | Differences in chemical composition between the phytoplankton-derived DOM. (a) Heatmap of the 111 compounds identified between the different phytoplankton species. Data were log-transformed and mean centred. An interactive version of this figure is available (Fig. S2).

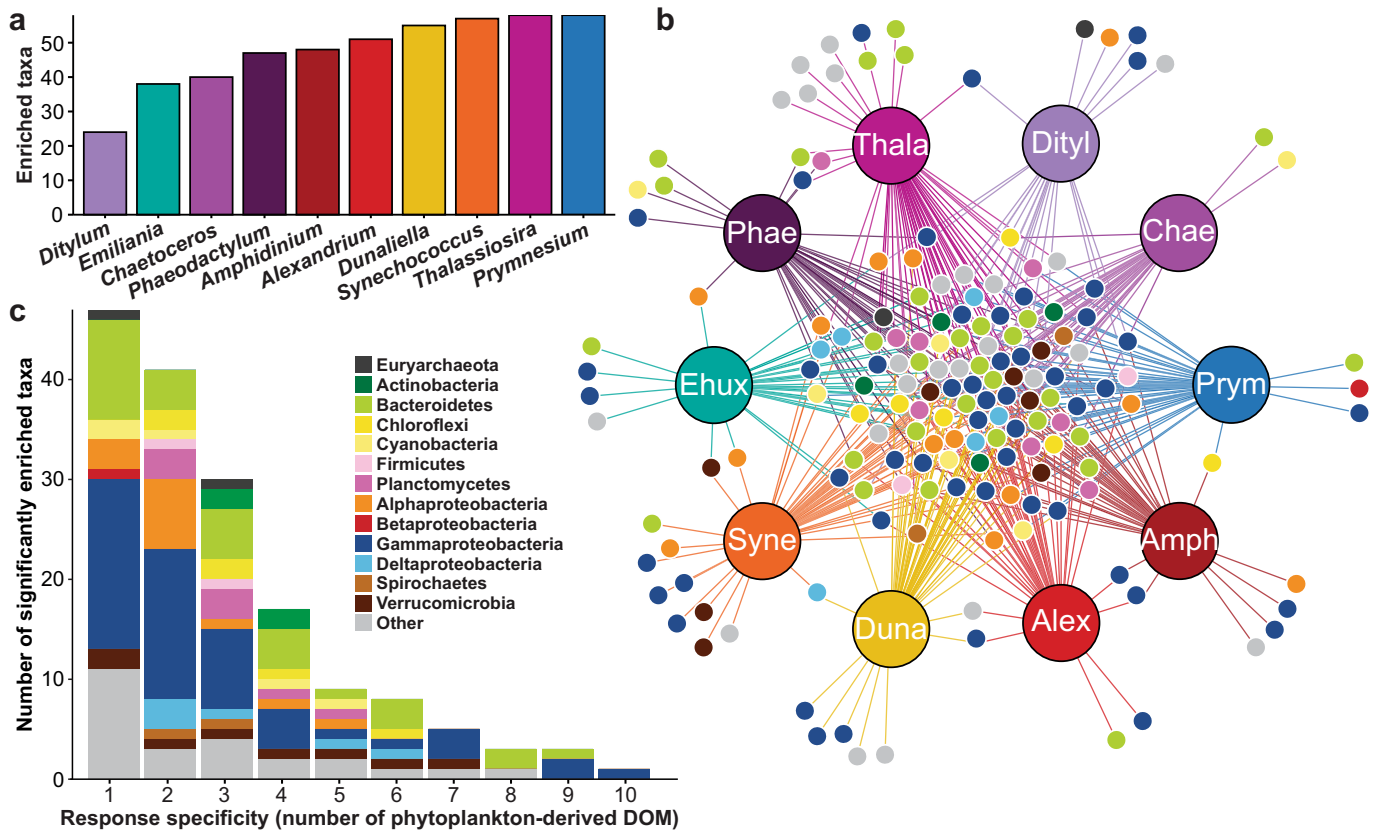
(b) Principal component analysis (PCA) of chemical composition of the phytoplankton-derived DOM: displaying the top three components (explaining 64.7% of the variance).

Article



Extended Data Fig. 4 | Relative abundance of the prokaryotic families present in the bulk seawater, the FSW controls, and in the different phytoplankton-derived DOM. Only taxa representing more than 2% of the

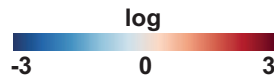
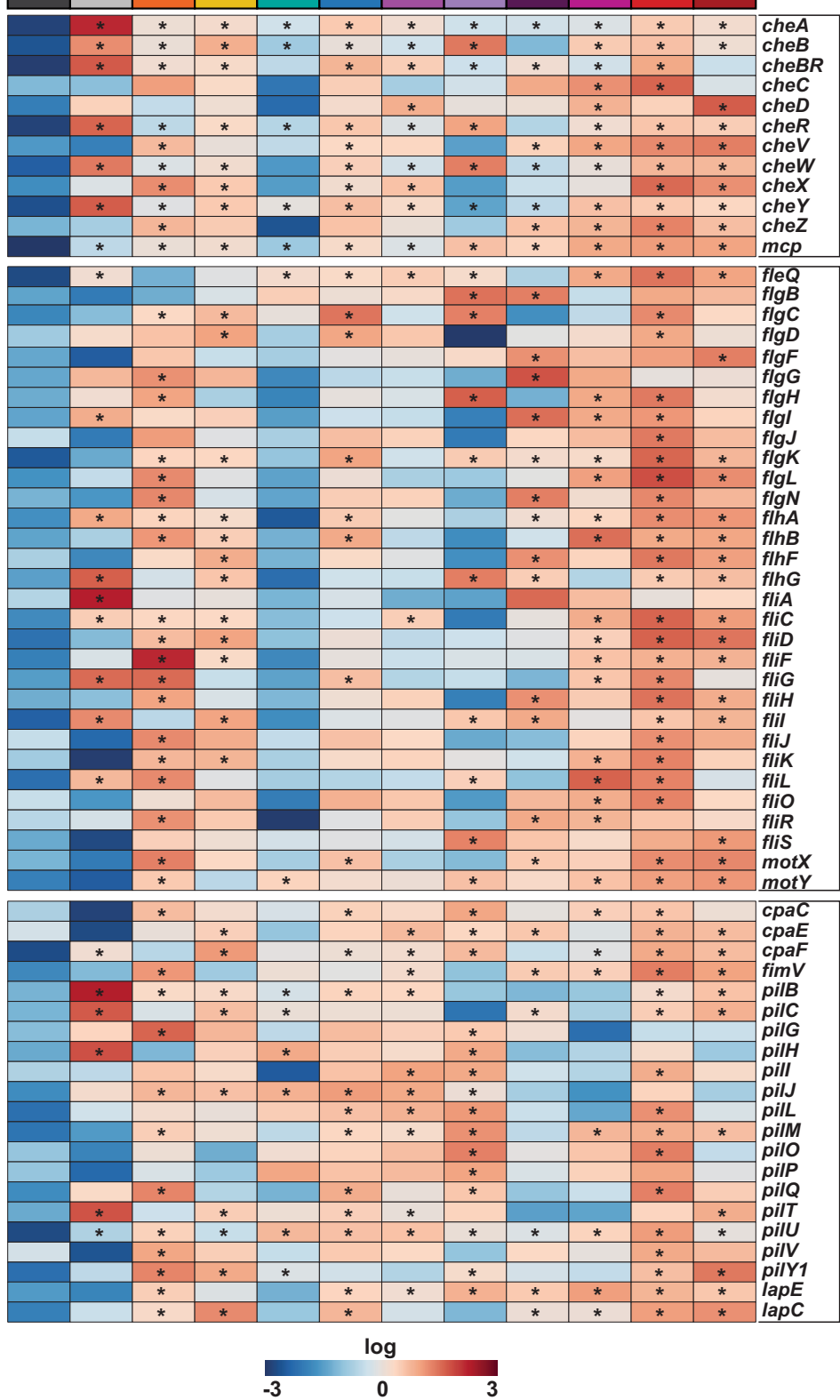
communities are displayed in colours, those representing less than 2% and grouped as “Other”. ND: taxonomy not determined at the family level.



Extended Data Fig. 5 | Prokaryotic taxa significantly enriched the phytoplankton-derived DOM treatments. (a) Number of prokaryotic taxa enriched in each phytoplankton-DOM treatment (compared to filtered seawater controls). The full list of taxa significantly enriched in phytoplankton-derived DOM treatments can be found in Supplementary Table 6. (b) Network analysis showing the differentiation between “generalist” and “specialist” families at the taxonomic level. This network has the same

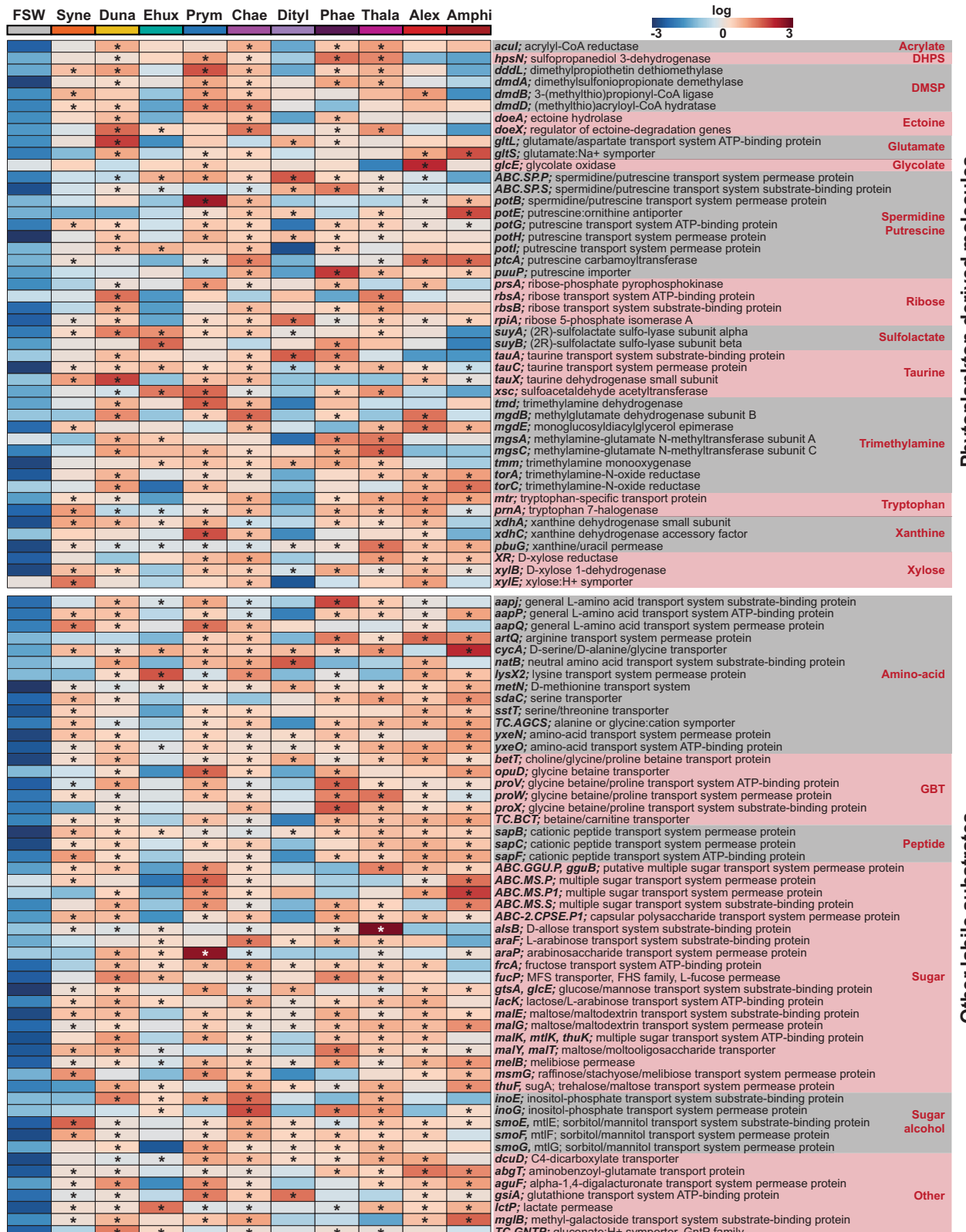
topology than the Figure 2b. Chemotactic prokaryotic taxa (small circles; nodes) are linked to the treatments they responded to (large circles) by lines with colours corresponding to each treatment. Each node is colour coded based on its taxonomy. (c) Number of prokaryote taxa significantly enriched in one or more phytoplankton-derived DOM treatments (compared to filtered seawater controls). Another graphical representation of this data can be found in Figure 2b.

Bulk FSW Syne Duna Ehux Prym Chae Dityl Phae Thala Alex Amphi



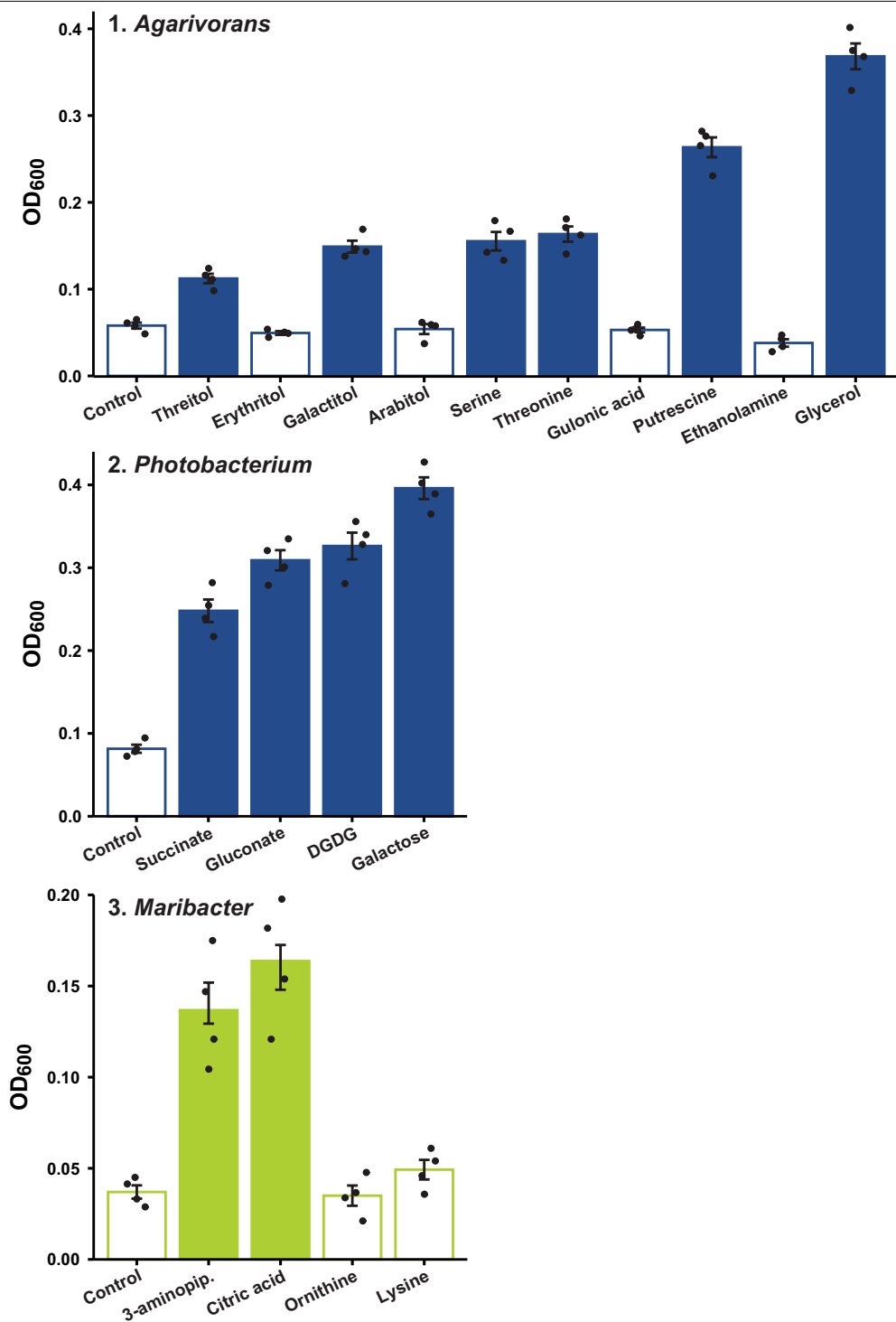
Extended Data Fig. 6 | Genes involved in motility, chemotaxis and surface-attachment were significantly enriched in the ISCA treatments compared to the bulk seawater. Data were log-transformed and

mean-centred ($n = 4$) for each ISCA treatment. Asterisks highlight significant enrichment compared to the bulk seawater (F-tests (one-sided), $p < 0.05$).



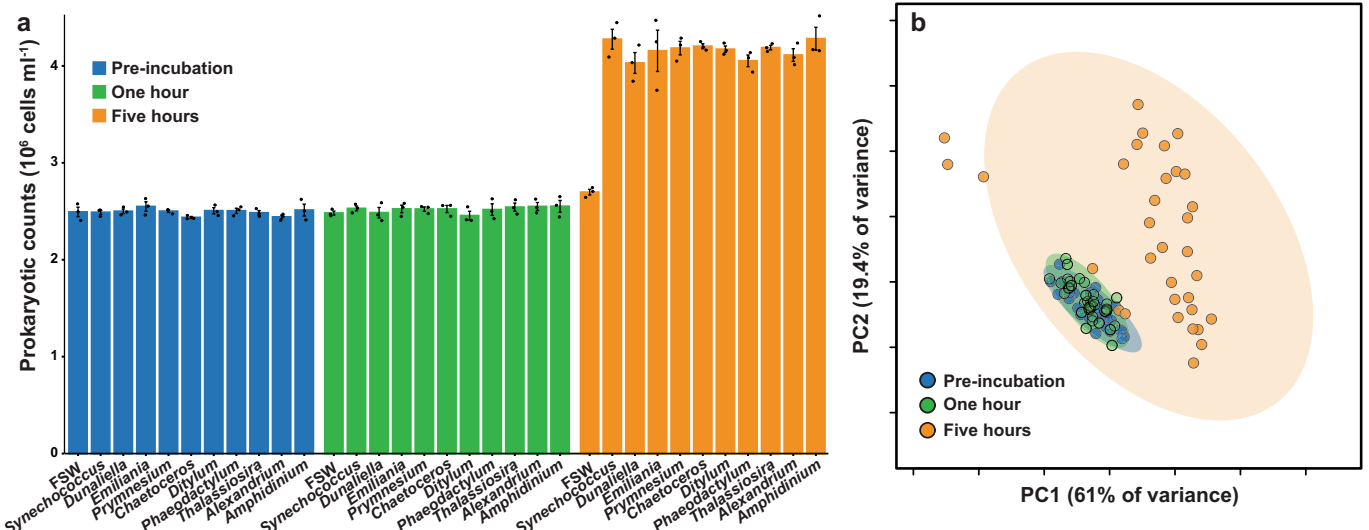
Extended Data Fig. 7 | Genes involved in the uptake and degradation of phytoplankton-derived molecules (selected from the literature)^{39,67–70}, as well as in the transport of a range of labile substrates, were significantly enriched in the prokaryotic communities responding to phytoplankton-derived DOM. Data were log-transformed and mean-centred ($n = 4$) for each

ISCA treatment. Asterisks highlight significant enrichment compared to the FSW treatment (F-tests (one-sided), $p < 0.05$, all p -values are reported in Supplementary Table 8). DMSP: dimethylsulfoniopropionate; DHPS: 2,3-dihydroxypropane-1-sulfonate; GBT: Glycine betaine.



Extended Data Fig. 8 | Assay testing the ability of the bacterial isolates to catabolize the validated chemoattractants (Figure 4b). Each chemoattractant was inoculated at a concentration of 1 mM ($n = 4$) in an artificial seawater medium supplemented with 0.2% of casamino acids. After 48 h, the optical density (OD₆₀₀) of each culture was compared to controls

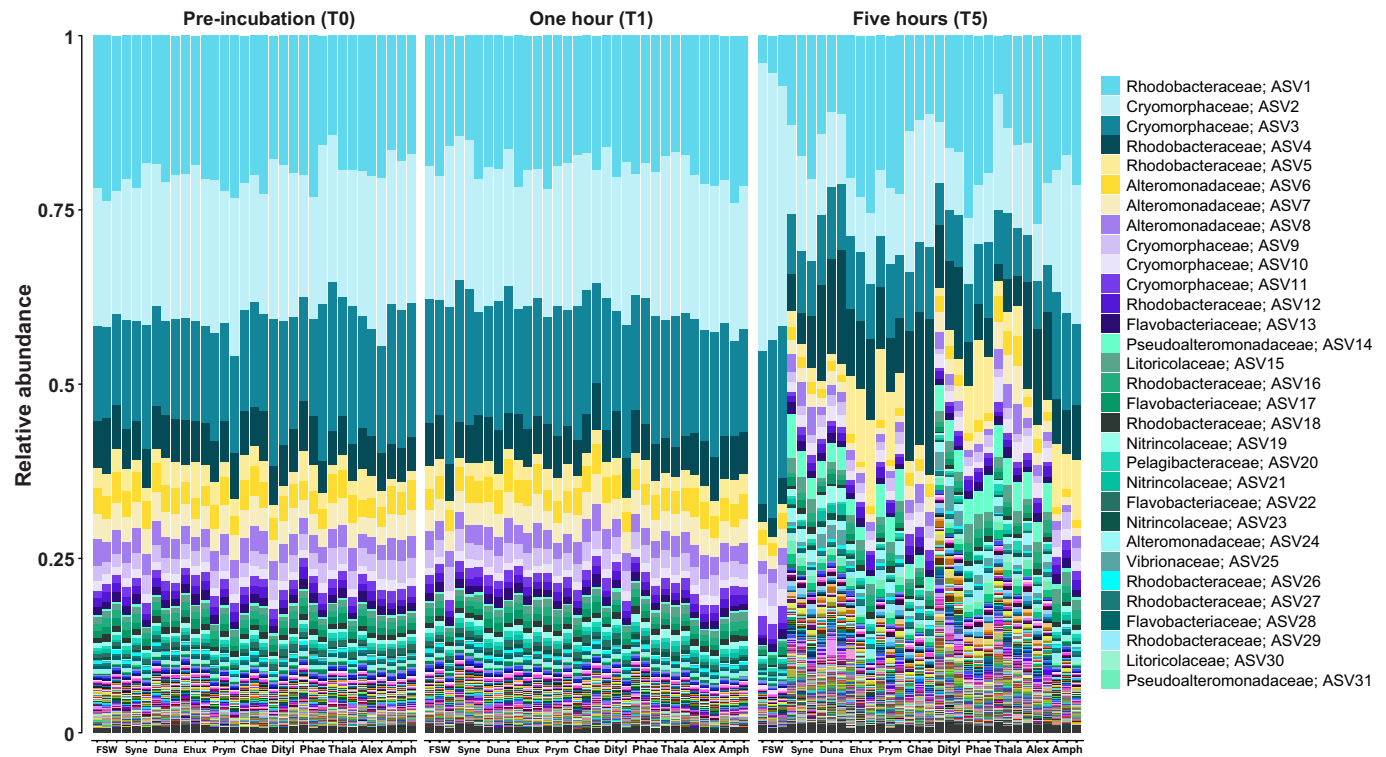
only containing casamino acids. DGDG: Digalactosyldiacylglycerol; 3-aminopip: 3-aminopiperidin-2-one. Solid bars are significantly different from wells containing FSW (ANOVA (one-sided), $p < 0.05$, all p -values are reported in Supplementary Table 9). Data are presented as mean values \pm SEM.



Extended Data Fig. 9 | Control for bacterial growth during the ISCA deployment time. (a) Comparison of prokaryotic cell counts before, and then 1 h and 5 h after post incubation with phytoplankton-derived DOM (1 mg mL^{-1}). The number of prokaryotic cells were not statistically different between pre-incubation and one hour of incubation (ANOVA (one-sided), $n = 3$, $p = 0.8026$). Data are presented as mean values \pm SEM. (b) Principal component analysis (PCA) of bacterial community composition resulting from incubations

(explaining 80.4% of the variance), revealing the overlap between bacterial community compositions pre-incubation and those after 1 h of incubation. An analysis of similarities confirmed that community compositions were not significantly different pre-incubation and after one hour of incubation (ANOSIM; 99,999 permutations; $n = 33$; $R = 0.108$; $p = 0.2$), but significant differences were observed after five hours ($R = 0.602$; $p = 0.001$).

Article



Extended Data Fig. 10 | Control for shifts in bacterial composition during the ISCA deployment time. Relative abundance of the bacterial communities (at the ASV level) before, 1 h and 5 h of incubation with phytoplankton-derived DOM (1 mg mL⁻¹). The legend only shows the 30 most abundant ASVs.

Reporting Summary

Nature Research wishes to improve the reproducibility of the work that we publish. This form provides structure for consistency and transparency in reporting. For further information on Nature Research policies, see our [Editorial Policies](#) and the [Editorial Policy Checklist](#).

Statistics

For all statistical analyses, confirm that the following items are present in the figure legend, table legend, main text, or Methods section.

n/a Confirmed

- The exact sample size (n) for each experimental group/condition, given as a discrete number and unit of measurement
- A statement on whether measurements were taken from distinct samples or whether the same sample was measured repeatedly
- The statistical test(s) used AND whether they are one- or two-sided
Only common tests should be described solely by name; describe more complex techniques in the Methods section.
- A description of all covariates tested
- A description of any assumptions or corrections, such as tests of normality and adjustment for multiple comparisons
- A full description of the statistical parameters including central tendency (e.g. means) or other basic estimates (e.g. regression coefficient) AND variation (e.g. standard deviation) or associated estimates of uncertainty (e.g. confidence intervals)
- For null hypothesis testing, the test statistic (e.g. F , t , r) with confidence intervals, effect sizes, degrees of freedom and P value noted
Give P values as exact values whenever suitable.
- For Bayesian analysis, information on the choice of priors and Markov chain Monte Carlo settings
- For hierarchical and complex designs, identification of the appropriate level for tests and full reporting of outcomes
- Estimates of effect sizes (e.g. Cohen's d , Pearson's r), indicating how they were calculated

Our web collection on [statistics for biologists](#) contains articles on many of the points above.

Software and code

Policy information about [availability of computer code](#)

Data collection Trimmomatic v0.36, CytExpert Version 2.4, Agilent MassHunter Qualitative and Quantitative Analysis version B.08.00

Data analysis MetaboAnalyst 4.0 for metabolomic analyses; GraftM v0.11.1 for taxonomic profiling of metagenome reads; DIAMOND v0.9.22 for reads quality control; PRIMER (v6.1.14) for community analyses; Dada2 version 1.22.0 was used to analyse amplicon sequencing data, the R packages MetagenomeSeq version 1.26.3 was used for statistical analyses. All custom analysis scripts are available on GitHub (<https://github.com/JB-Raina-codes/ISCA-paper>).

For manuscripts utilizing custom algorithms or software that are central to the research but not yet described in published literature, software must be made available to editors and reviewers. We strongly encourage code deposition in a community repository (e.g. GitHub). See the Nature Research [guidelines for submitting code & software](#) for further information.

Data

Policy information about [availability of data](#)

All manuscripts must include a [data availability statement](#). This statement should provide the following information, where applicable:

- Accession codes, unique identifiers, or web links for publicly available datasets
- A list of figures that have associated raw data
- A description of any restrictions on data availability

The raw fastq read files were deposited in Sequence Read Archive (SRA) (accession number: PRJNA639602).

The 16S rRNA gene sequences of the two isolates were deposited in GenBank (accession numbers: MT826233-MT826234 and MZ373175).

The 16S Amplicon sequences were deposited in SRA (accession number: PRJNA707306).

The metabolomes were deposited in MetaboLights (accession number: MTBLS1980). All other source data are provided with this paper.

Field-specific reporting

Please select the one below that is the best fit for your research. If you are not sure, read the appropriate sections before making your selection.

- Life sciences Behavioural & social sciences Ecological, evolutionary & environmental sciences

For a reference copy of the document with all sections, see nature.com/documents/nr-reporting-summary-flat.pdf

Ecological, evolutionary & environmental sciences study design

All studies must disclose on these points even when the disclosure is negative.

Study description

This study involved the characterisation of prokaryotic chemotaxis response *in situ*. We deployed our In Situ Chemotaxis Assays (ISCA) at a coastal site and quantified the chemotactic response for 10 different treatments and compared each to a control. Each experiment was replicated across four different ISCA. The study was a one-factor design.

Research sample

The research samples consisted of seawater from a coastal site and containing natural communities of marine microorganisms. The study site is located less than 10 km from a fully equipped laboratory, which allowed the direct processing of the samples, repeated sampling and the completion of experiments.

Sampling strategy

Replicates In Situ Chemotaxis Assays (ISCA) were deployed simultaneously in coastal seawater near Sydney, Australia. Devices were deployed at a depth of one meter for an hour. Samples were then collected from the ISCA for the various downstream analyses. Pilot studies were carried out at the field sites prior to conducting the experiment described in this manuscript. We selected our sample size based on these pilot studies, the available literature, feasibility and the level of variability between replicates. No statistical methods were used to predetermine sample size.

Data collection

ISCA samples were collected *in situ*, and either snap frozen or chemically fixed. Temperature, pH, salinity and oxygen concentrations were also recorded *in situ* (using pen and paper) and entered in a spreadsheet upon return from the field. Nutrient data were recorded electronically on an Aquakem analyser (Thermo Scientific). Cell counts data were recorded electronically using CytExpert Version 2.4. Mass spectra were collected electronically using a 7890A Agilent gas chromatograph and a 5975C Agilent quadrupole mass spectrometer (Agilent, Santa Clara, USA). Metagenomic data were collected electronically following sequencing on an Illumina NextSeq 500 platform. Amplicon data were collected electronically following sequencing on an Illumina MiSeq platform.

Timing and spatial scale

Twelve field experiments took place between April 2016 and March 2018 to take into account the effect of different environmental variables on the prokaryotic chemotactic responses. The same coastal site was repeatedly sampled during these experiments (Clovelly Beach).

Data exclusions

No data was excluded from the study and analyses.

Reproducibility

All *in situ* experiments described in our study are fully replicated environmental sampling campaigns carried out at different times and/or different years. The first four *in situ* experiments (April to August 2016) were carried out using three ISCA replicates while the last eight experiments (December 2016 to March 2018) were carried out using four ISCA replicates. The laboratory chemotaxis assays were also carried out using four ISCA replicates. All the control tests for the ISCA deployment times were carried out in triplicates.

Randomization

Treatment positions were fully randomised within the In Situ Chemotaxis Assay. Samples were recruited *in situ* from seawater and were therefore not preallocated into experimental groups.

Blinding

Blinding was not pertinent to our study because it did not include any animals and/or human research participants. In addition, blinding was not possible since many analyses were also carried out by the persons in charge of sampling.

Did the study involve field work? Yes No

Field work, collection and transport

Field conditions

The field conditions are described in Supplementary Table 2.

Location

Field deployments were carried out between April 2016 and March 2018 at Clovelly Beach (33.91°S, 151.26°E), a coastal location near Sydney, on the eastern coast of Australia.

Access & import/export

No permit was required to carry out the fieldwork.

Disturbance

No disturbance to the ecosystem was caused by this study.

Reporting for specific materials, systems and methods

We require information from authors about some types of materials, experimental systems and methods used in many studies. Here, indicate whether each material, system or method listed is relevant to your study. If you are not sure if a list item applies to your research, read the appropriate section before selecting a response.

Materials & experimental systems

n/a	Involved in the study
<input checked="" type="checkbox"/>	Antibodies
<input checked="" type="checkbox"/>	Eukaryotic cell lines
<input checked="" type="checkbox"/>	Palaeontology and archaeology
<input checked="" type="checkbox"/>	Animals and other organisms
<input checked="" type="checkbox"/>	Human research participants
<input checked="" type="checkbox"/>	Clinical data
<input checked="" type="checkbox"/>	Dual use research of concern

Methods

n/a	Involved in the study
<input checked="" type="checkbox"/>	ChIP-seq
<input type="checkbox"/>	Flow cytometry
<input checked="" type="checkbox"/>	MRI-based neuroimaging

Flow Cytometry**Plots**

Confirm that:

- The axis labels state the marker and fluorochrome used (e.g. CD4-FITC).
- The axis scales are clearly visible. Include numbers along axes only for bottom left plot of group (a 'group' is an analysis of identical markers).
- All plots are contour plots with outliers or pseudocolor plots.
- A numerical value for number of cells or percentage (with statistics) is provided.

Methodology

Sample preparation

Seawater samples derived from the In Situ Chemotaxis Assay were fixed (2% glutaraldehyde, final concentration), kept on ice and analysed the same day. Each sample was then stained with SYBR Green (1:10,000 final dilution; ThermoFisher), incubated for 15 min in the dark and analysed.

Instrument

CytoFLEX S (Beckman Coulter, USA) using filtered MilliQ water as sheath fluid.

Software

CytExpert Version 2.4

Cell population abundance

The bacterial cell population was the only one present in the analysis plots.

Gating strategy

Gating around the bacterial population was determined by analysing bulk seawater.

- Tick this box to confirm that a figure exemplifying the gating strategy is provided in the Supplementary Information.